TAMPEREEN TEKNILLINEN YLIOPISTO

MIKKO KOSKI

DEVELOPMENT OF A NOVEL HIGH RESOLUTION OPTICAL NEUROIMAGING METHOD

Master of Science Thesis

Examiners: Professor Ari Visa, D.Sc.
(Tech.) Jarno M. A. Tanskanen

Examiners and topic approved in the
Computing and Electrical Engineering
Faculty Council meeting on 3rd Mar 2010

TIIVISTELMÄ

TAMPEREEN TEKNILLINEN YLIOPISTO
Sähkötekniikan koulutusohjelma
KOSKI, MIKKO: Uuden optisen suuriresoluutioisen hermokuvantamismenetelmän kehitys
Diplomityö, 64 sivua, 3 liitesivua
Lokakuu 2010
Pääaine: Signaalinkäsittely
Tarkastajat: Professori Ari Visa, TkT Jarno M. A. Tanskanen
Avainsanat: Hermokuvantaminen, mikroskooppikuvantaminen, nopea luontainen optinen signaali, mikroelektrodimatriisi, hermoverkot

Tämän diplomityön tarkoituksena oli toteuttaa uusi suuriresoluutioinen in vitro –kuvantamismenetelmä hermosolujen aktiivisuuden mittaamiseksi soluviljelmistä. Suuren aika- ja paikkaresoluution omaavat hermokuvantamismenetelmät tarjoavat hyödyllistä informaatiota tutkittaessa toiminnallisia hermoverkkoja ja niissä tapahtuvaa informaation käsittelyä.

Suuriresoluutioisia kuvantamismenetelmiä hermokudoksen toiminnan seuraamiseen on kehitetty. Nämä menetelmät pohjautuvat fluoresenssiin, joka saadaan aikaan käyttämällä fluoresoivia väriaineita, jotka ovat kuitenkin soluille haitallisia. Työssä tutkittu uusi menetelmä pohjautuu sitä vastoin hermokudoksen luonnolliseen toiminnallisuuteen, eikä fluoresoivia väriaineita tarvita. Menetelmä hyödyntää valomikroskoopilla havaittavia dynaamisia optisia signaaleja, jotka aiheutuvat luonnollisista muutoksista hermokudoksen optisissa ominaisuuksissa aktiopotentiaalin aikana.

Tehdyn kirjallisuuskatsauksen pohjalta työssä on kattavasti esitetty aiheeseen liittyvä teoria. Aiemmissa tutkimuksissa optisia signaaleja on onnistuttu mittaamaan, mutta mittaukset on tehty käyttäen yksittäisiä valodiodeja. Tässä työssä käytetään yksittäisen valodiodin sijasta suuren pikselimäärän omaavaa digitaalista kuvantamissensoria, jotta hermoverkon toiminnaalisuudesta saataisiin spatiaalinen kuva. Aikaisempia vastaavia tutkimuksia suuriresoluutioisella sensorilla ja vastaavalla hermokudostyypillä ei kirjallisuusselvityksessä löytynyt.

Työhön liittyvät mittaukset suoritettiin kuvantamalla ja samanaikaisesti sähköisesti mittaamalla ihmisalkion kantasoluista erilaistettuja hermosoluja ja niiden muodostamia toiminnallisia hermoverkkoja. Kuvantaminen suoritettiin mikroskooppiin liitetyllä tieteelliseen kuvantamiseen soveltuvalla CCD sensorilla, ja sähköiset mittaukset mikroelektrodimatriisilaitteistolla (MEA). Koska MEA tarjoaa sähköisistä mittauksista paikkainformaatiota, tätä käytettiin hyväksi todentamaan kuvista tehdyt havainnot ja siis menetelmän toimivuus.

Mittaukset ja näin ollen myös uuden kuvantamismenetelmän käytännön kehitys kuitenkin epäonnistuivat johtuen käytössä olleen laitteiston soveltumattomuudesta tähän vaativaan tehtävään, erityisesti johtuen mikroskoopin ja sen valaistuksen huonosta kunnosta, jolle ei kuitenkaan tämän työn puitteissa voitu tehdä mitään.

Työssä perehdyttiin kuitenkin syvällisesti aiheena olleeseen kuvantamismenetelmään, sen teoriaan ja vaatimuksiin, sekä laadittiin suunnitelma kuvantamisen toteuttamiseen vaadittavasta laitteistosta sekä itse menetelmästä. Tämän työn pohjalta laitteiston salliessa pitäisi suunnitellun kuvantamisen olla suoraviivainen tehtävä.

ABSTRACT

TAMPERE UNIVERSITY OF TECHNOLOGY
Master's Degree Programme in Electrical Engineering
KOSKI, MIKKO: Development of a novel high resolution optical neuroimaging method
Master of Science Thesis, 64 pages, 3 appendix pages
October 2010
Major: Signal processing
Examiner: Professor Ari Visa, D.Sc. (Tech.) Jarno M. A. Tanskanen
Keywords: Neuroimaging, microscope imaging, fast intrinsic optical signals, microelectrode array, neuronal networks

The purpose of this thesis was to develop new high resolution neuroimaging method, which allows detection of neuronal activity from neuronal tissue samples in laboratory conditions. Neuroimaging methods utilizing high spatial and temporal resolution provide highly useful information about the functioning and information processing especially in functional neuronal networks.

High resolution neuroimaging methods for monitoring the functioning of neuronal tissue have been developed. These methods are based on the specimen fluorescence, which is achieved by using fluorescent dyes, which are harmful for the cells. However, the studied new neuroimaging method is based purely on the natural functioning of the neuronal tissue, without using any dye substances. Method utilizes the microscope observations of fast intrinsic optical signals (FIOS), which arise from the natural action potential induced changes in the optical properties of the neuronal cells.

Based on the literature review, in which some successful FIOS measurements were found, the theories concerned with the work are thoroughly described in this thesis. However, earlier measurements employed only single photodiode elements. In this thesis, the single photodiode element is replaced by digital imaging sensor, which is able to provide spatial image of the functioning of the neuronal network. Regardless of the extensive literature search, no earlier studies with high resolution sensor and using same type of specimens were found.

The measurements related to this thesis were conducted by simultaneously imaging and electrically measuring functional networks of neuronal cells derived from human embryonic stem cells. Imaging was conducted using optical light microscopy equipped with a scientific grade CCD imaging sensor, whereas electrical measurements were conducted using microelectrode array (MEA) technique, which provided spatial measuring information. MEA data was used to verify the imaging results and thus the functioning of the developed method.

The measurements and the development task of this new neuroimaging method failed primarily due to the bad condition of the imaging equipment, especially the microscope and the illumination used. Unfortunately, it was not possible to fix these issues within the resources allocated for this thesis.

However, this thesis focused to cover thoroughly the theory of the studied imaging method and the requirements related to it. Also a plan was made for the required imaging equipment as well as for implementing the method itself. Based on this thesis and with proper devices, the proposed imaging method should be straightforward to implement.

PREFACE

This thesis was done for the Department of Biomedical Engineering of Tampere University of Technology. First of all, I would like to thank Professor Jari Hyttinen, the head of the department, who showed great interest towards this thesis project and arranged the funding for me to concentrate completely on this project.

Additionally, I would like to express my gratitude to my thesis instructor and examiner, D.Sc. Jarno M. A. Tanskanen. He has given me a lot of useful advice and helped me with a great attitude during this thesis process. Especially I would like to thank him for giving me the insight into the academic world, due to his own enthusiasm related to several scientific areas. I would like to thank also my other examiner, Professor Ari Visa from the Department of the Signal Processing, who also gave me useful advice on how to approach the research problem of this thesis.

The measurements related to this thesis, which were conducted in the Regea Institute for Regenerative Medicine, would not have been possible without the help of Laura Ylä-Outinen and Juha Heikkilä from the Regea, who both helped me to get familiar with the measuring equipments and environment. Especially Juha helped me a lot, by doing the specimen preparations and helping in the conduction of the measurements. So big thanks to both of them.

Huge thanks belong to my good friends and fellow students, Markus and Tomi. Together with these guys, I have struggled through the numerous assignments, exams and nearly everything related to the studies in Tampere University of Technology. Now it is finally the time to graduate.

Last but not least, the biggest thanks I would like to devote to my common-law wife, Suvi. She has been there for encouraging me during good times as well as hard times not related just to this thesis, but my life overall. I am very grateful for her love towards me.

13.10.2010, Tampere

Mikko Koski

TABLE OF CONTENTS

ABBREVIATIONS, TERMS AND SYMBOLS

Abbreviations

ADC	Analog-to-digital converter. Digitization unit consisting of electrical components that convert electrical charge to voltage levels which are interpreted as discrete digital values.
CCD	Charge-coupled device. Digital imaging sensor architecture.
CMOS	Complementary metal oxide semiconductor. Another digital imaging sensor architecture.
FIOS	Fast intrinsic optical signals. Optical signals that arise from neuronal tissue during action potential.
fps	Frames per second. Defines frame rate of digital imaging sensor.
hESC	Human embryonic stem cell. Cell type that can develop to nearly any other cell type found in human body.
LED	Light emitting diode. A semiconductor based light source.
MEA	Microelectrode array. A measurement platform made of glass, where measuring electrodes are embedded in the form of an array.
MOS	Metal oxide semiconductor. Photosensitive component used as a pixel in CCD sensors.
OCT	Optical coherence tomography. Interferometric optical imaging method.
ROI	Region of interest. Chosen sub-region in the entire image area.
SNR	Signal-to-noise ratio. Defines signal quality by comparing it to the noise contribution.

Terms

In vitro	Experiment conducted outside a living organism in an artificial environment, as opposed to *in vivo* conditions.
In vivo	Experiment conducted with an entire living organism, as opposed to *in vitro* conditions.
Birefringence	Double refraction property of a material exhibiting optical anisotropy.
Retardation	Phase difference of two light waves propagating with different velocities.

Symbols

η	Refractive index of material
c	Speed of light in vacuum
v	Speed of light in a material
$\Delta\varphi$	Phase shift of light
φ	Phase of light
λ	Wavelength of light
d	Diameter of the phase object
V	Membrane potential
$\Delta\eta$	Refractive index difference between two materials
η^n	Refractive index change related to the membrane potential V and thickness d of the membrane
η_e	Refractive index of the extraordinary light ray polarized parallel to the optical axis in the birefringent material
η_o	Refractive index of the ordinary light ray polarized perpendicularly to the optical axis in the birefringent material
I	Image to be processed in the activity detection algorithm
$I_{reference}$	Reference image used to calculate the difference image ΔI in the activity detection algorithm
ΔI	Difference image obtained from the activity detection algorithm

1. INTRODUCTION

Traditional neuroimaging methods focus to explore brain as a spatial and functional structure. At the moment, these techniques require relatively expensive and complex devices. Additionally these methods suffer from relatively poor temporal resolution, because they do not directly measure the neuronal activity itself but the events occurring as a consequence of neuronal activity, like increased blood flow and blood oxygenation in certain areas of the brain. For example, functional magnetic resonance imaging, which is one of the most used neuroimaging method nowadays, is based on those hemodynamic changes in the brains. Neuroimaging methods with temporal resolution matching better the time course of single neuronal events, the action potentials, would provide much more detailed information about the functioning of neuronal tissue.

These kinds of neuroimaging methods have been developed for the *in vitro* experimental studies, where action potential generation and propagation between single neuronal cells can be traced with high temporal and spatial resolution by using high performance digital imaging sensors and sophisticated image processing methods. However, the existing methods are based on the sample fluorescence, which is initiated by using fluorescent marker substances like voltage sensitive dyes for example, which change their fluorescent characteristics due to the changing membrane potential of the neurons during neuronal activity **[16]**. Although these methods are widely used in experimental neurosciences nowadays, the fact that fluorescent dyes are generally harmful by nature restricts their applicability and allows them to be used only in experimental studies.

In this thesis, a new high resolution optical neuroimaging method is proposed. The method allows for the detection of neuronal activity from *in vitro* neuronal tissue samples and cultures with relatively simple measuring devices and methods, and without using any kinds of marker substances. In other words, the neuronal tissue is not modified and its functioning is not altered in any way. Thus, compared to traditional fluorescence based methods, this method could be freely utilized also in clinical *in vivo* applications with human subjects. The method is based on so called fast intrinsic optical signals (FIOS), which are optical signals arising from the action potential induced changes in the optical properties of the neuronal cells. These signals were first discovered already over 60 years ago in photodiode measurements, where the changes of transmitted light intensity through a stimulated nerve correlated tightly with the action potentials measured simultaneously with extracellular electrodes [**1**].

The purpose of the work presented in this thesis is to study the possibility to develop a high resolution FIOS imaging method, which is able to detect neuronal activity from neuronal tissue, by utilizing a basic optical light microscope equipped with a high per-

formance CCD imaging sensor. The development task includes experiments that are conducted by imaging spontaneously active cultured neuronal networks. The specimens consist of neurons derived from human embryonic stem cells (hESCs), which start to form functional neuronal networks during their maturation process. These neuronal networks are cultured on microelectrode arrays (MEAs), which allow simultaneous measurement of electrophysiological activity and imaging. The MEA itself is a relatively new and sophisticated method to measure electrical activity, which also provides coarse spatial measuring resolution. Although this spatial resolution is decades from that of optical imaging, it is highly useful in the development process and due to this, the MEA information is used to verify the imaging results.

Although some research records related to the area of FIOS can be found, the underlying physical mechanisms still remain unconfirmed. The reason for this might be the relatively small amount of relevant research related to this area, which in turn might be due to the difficulty of detecting these signals, which requires sophisticated and highly sensitive imaging equipments. However, the recent developments of the optical imaging techniques, especially the performance and sensitivity of the digital imaging sensors, enable easier detection and measurement of these elusive optical signals. However, this thesis is the first attempt to measure the activity of single neuronal cells and spontaneously active neuronal networks by using basic optical light microscopy and a high resolution CCD imaging sensor. If successfully conducted, this thesis provides a very powerful and still simple method for detecting the activity from any kind of *in vitro* neuronal tissue. Furthermore, it is not unimaginable that the method might become applicable also in *in vivo* studies and in clinical applications.

Although the purpose of this thesis is to study the imaging aspect, a large effort is focused to explore the backgrounds related to the optical signals and their generation in neuronal tissue. By knowing the backgrounds related to the physical and physiological mechanisms, the detection of these signals can be improved, especially by applying special light microscopy techniques, which improve the performance of the basic light microscope. Thus, large part of the contents of this thesis focuses to introduce the theory of FIOS based on the literature. In addition, the biological backgrounds of neuronal tissue and its functions are covered, as well as the theory related to the optical and electrical signal acquisition and the acquisition devices used in the measurements. The rest of this thesis focuses on analyzing the measurement results and discusses the problems related to the currently available equipment and the development process. Based on the discussion, improvements for the possible future work are proposed, and finally in the conclusions, the feasibility of the proposed neuroimaging method is discussed.

2. NEURONS AND NEURONAL NETWORKS

In this chapter, the relevant biological background of the neuronal tissue is presented. The discussion mainly focuses to cover the neuronal physiology, but also some anatomical aspects are explored. The chapter starts by introducing the basic structure of the neurons and neuronal tissue, and thereafter continues to explore the elemental mechanism of action potential. At the end of the chapter, the concept of functional neuronal networks is briefly introduced.

2.1. Neuron

Neurons are the basic components of the nervous system, which are specialized to receive and transmit information in the nervous system. Nervous system itself is responsible of sensing and controlling every living organism. Basic operational function of the nervous system is to gather information (sensory input) about changes in the organism and its environment (stimuli), and generate a desired response or effect (e.g., motor output) based on processing of the collected information [**2**]. The capability of the nervous system to communicate and control actions is based on the ability of the neurons to rapidly conduct electrical impulses from one part of the body to another by using a signaling mechanism called the action potential, which also forms the basis of information processing the in the brain.

The nervous system consists of several types of neurons, but all of them have a common basic structure, which is composed of the cell body and the processes [**2**]. The cell body is often called the soma, which is responsible of the metabolic needs of the cell. From the cell body originate the processes, axons and dendrites, which are responsible of receiving and transmitting the electrochemical signals. Functional difference between the axons and dendrites is that dendrites conduct the incoming messages, while axons conduct messages away from the soma. In other words, axon is literally the output of the nerve cell, while dendrites play the role of the inputs. In addition to this functional difference, one neuron can have hundreds of branching dendrites, whereas there is always only one axon. Figure 2.1 illustrates the general structure of a neuron.

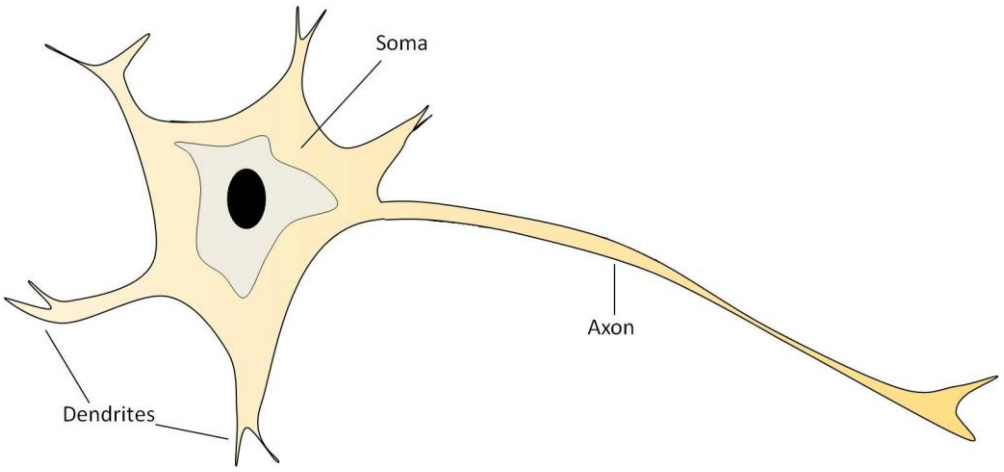

Figure 2.1. *General structure of a neuron. From the soma, originate several branching dendrites, which are responsible to collect action potential stimulus from other neurons.*

Like any other cell type, neurons have a cell membrane that separates the cell cytoplasm from the surroundings and which structure consists of two layers of phospholipids. This lipid bilayer has also membrane proteins embedded on it, which are used, e.g., as ion transferring channels between the cell cytoplasm and the extracellular fluid. [**2**] Although the general structure of the neuron cell membrane is similar that of any other cell, it is due to the special functioning of the ion channels that the neuron is able to be the messenger of the nervous system.

2.1.1. Action potential

Primary function of the neuron is to process signals and to transmit them to other neurons. This signal is called an action potential, and the receiving and transmission process of the nerve impulse is called electrochemical signaling [**2**]. By electrochemical we mean that part of the signaling procedure happens electrically and part chemically. The chemical part of the signaling occurs at the end of the axon, where the tip of the axon, called axon terminal, forms a connection with the soma or the dendrite of the adjacent neuron. This connection is called a synapse. When the action potential arrives at the synapse, the transmitting neuron releases chemical neurotransmitter molecules into the synaptic cleft, which bind to receptors of the receiving membrane of the postsynaptic neuron. When neurotransmitters are bind to the receptors, ion channels open on the cell membrane and allow the inflow and outflow of the charged ions. This electric part of the signaling occurs in the axons and dendrites of the neuron, and it is based on the property of the cell membrane to change its permeability to sodium (Na+), potassium (K^+) and some other ions, e.g., due to the chemical signaling at the synapse or the propagating action potential. This electric current has its characteristic features, which determine the generation and propagation of the action potential. These features are discussed next and illustrated in Figure 2.2.

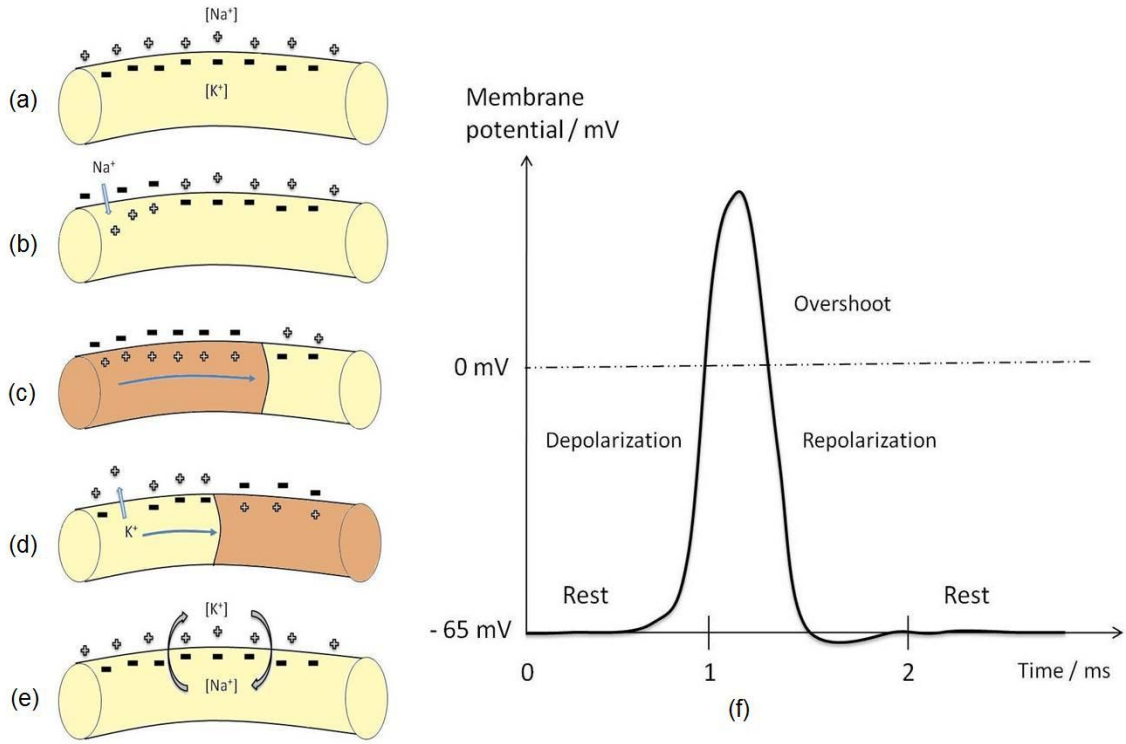

Figure 2.2. *The propagation of action potential in an axon. (a) – (e) Ion flow, i.e., electric current, across the cell membrane and the propagation of action potential. (f) Exemplary membrane potential during different phases of the action potential. Adapted from* [**2**] [**3**] .

At the resting state illustrated in Figure 2.2 (a), major positive ions outside the membrane are sodium ions, while the major positive ions inside the membrane are potassium ions. The potential difference at the resting state is about -65 mV, which is measured between the intracellular and extracellular space, i.e., over the cell membrane. The next phase in the action potential generation is the depolarization phase illustrated in Figure 2.2. (f), which is initiated by the incoming nerve stimulus (Figure 2.2 (b)). The changing membrane potential causes the sodium channels to open, and due to the large concentration gradient and electric potential difference, the sodium ions start to rush inside the cell and the potential difference start to decrease. This phase is called membrane depolarization, and if it exceeds a critical threshold value, the membrane launches the action potential. As illustrated in Figure 2.2 (c), depolarization spreads on the membrane, and the potential difference reaches its peak value of about +40 mV. The phase when the membrane potential is positive is called the overshoot. Immediately after the rapid depolarization phase, the permeability of the membrane changes again so that now in turn, the potassium channels open and potassium ions start to diffuse out of the neuron. This action is called the membrane repolarization, and it initiates the falling phase of the membrane potential curve (Figure 2.2 (f)), i.e., the membrane potential decreases, and finally restores the membrane potential back to the resting state. The membrane repolarization is illustrated in Figure 2.2 (d). Finally, the original ion concentrations inside and outside of the membrane are restored by the sodium-potassium pumps, which

transfer sodium ions out of the cell and potassium ions back in the cell, as illustrated in Figure 2.2 (e). It is to be noted that also many other ions and ion channels than those mentioned above participate in action potentials. [**2**] [**3**]

It is important to notice that one very characteristic property of the nerve impulse is the fact that, it is an all-or-nothing reaction. If the stimulus exceeds certain action potential threshold, the nerve impulse is always generated and it propagates rapidly through the entire axon, generally despite the length of it. The time course of an action potential as seen via an extracellular microelectrode is typically about 2 ms, which is the time that is needed for the membrane to go through the action potential phases described and illustrated in Figure 2.2. [**3**]

2.1.2. Neuronal network

To function as parts of the nervous system, neurons need to form functional and meaningful connections with each others. These connected neurons are called neuronal networks, which are essential structures for organized communication between single and groups of neurons. Development of network begins when neurons start to grow their axons and dendrites and when these processes form synaptic connections with other neurons [**4**].

During the development of a network, neurons start to spontaneously communicate using action potentials. This so called firing activity exhibits different and distinguishable patterns during the maturation of the network, from the spontaneous random firing of individual action potentials at the beginning of the development, to the spontaneous and synchronized spatially spreading firing activity at the mature stage of the neuronal network development [**4**] [**5**]. The studies of the development of the neuronal networks using novel techniques, like MEAs and high resolution optical neuroimaging methods, help exploring the dynamics of the functional neuronal networks in both spatial and temporal domains [**6**]. This increases the amount of important knowledge and understanding of how the brains process information, and provides better possibilities to treat physiological conditions like epilepsy or Alzheimer´s disease [**7**].

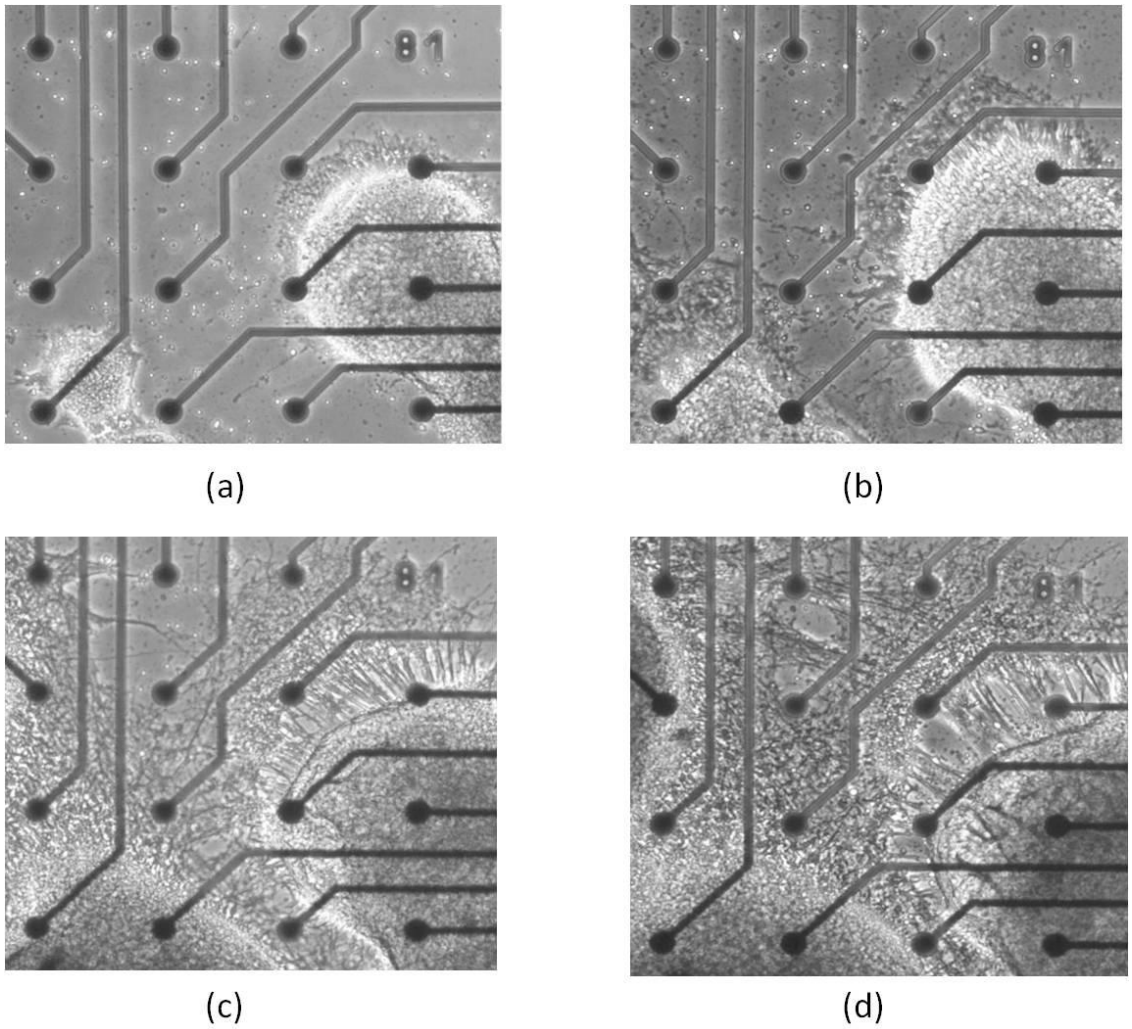

Figure 2.3. *Maturation process of a neuronal network cultured on MEA. (a) Network 1 day, (b) 6 days, (c) 11 days, and (d) 14 days after seeding.*

In Figure 2.3 is shown an example of a maturating neuronal network, which is used in the measurements related to this thesis. The formation and development of the neuronal network can be clearly seen by comparing the Figures 2.3 (a) - (d). In Figure 2.3 (a) there can be seen only neuronal cell aggregates, which are seeded on the MEA. During the maturation of the cell culture, neurons start to grow their processes, and in Figure 2.3 (d) the network has already developed so that it covers the whole electrode area shown.

3. DATA ACQUISITION

In this chapter the measuring devices related to the data acquisition process employed in this thesis are introduced. The chapter includes the discussion of optical signal acquisition consisting of the microscope and digital image acquisition, as well as the acquisition of electrophysiological signals. However, the focus is on the imaging aspects. The chapter begins by introducing the basics of optical microscopy and special microscopy techniques used in the measurements. After that follows the discussion of the digital image acquisition. In the end of this chapter, electrical signal acquisition is discussed.

3.1. Microscopy

The optical light microscope (also called brightfield or brightfield illumination microscope) is a widely used instrument in several areas of science, where closer examination of particles and structures of objects is important. The light microscopy is based on the simple principle of a magnifying lens system, and it basically consists of four components: a light source, condenser lens, objective lens and an eyepiece [**8**]. The light from the source is focused onto the specimen by the condenser lens and from there it is further focused and magnified onto the eyepiece by objective lens.

Although the basic principle of light microscope is very simple, it can be modified with variety of techniques, which improve its properties and performance. One such technique, which is used in this thesis, is the phase contrast microscopy, which is very useful when specimens under examination are nearly transparent, like in the case of biological samples, e.g., neuronal cells. The phase contrast microscopy is discussed in next section.

3.1.1. Phase contrast microscopy

The phase contrast microscopy is a technique, which has been developed to overcome the problem of lack of contrast of specimens, which do not absorb much light. Using ordinary light microscope, this kind of specimens appear nearly, because light passing through the specimen does not experience any amplitude variations. However, there occur alterations in phase of light waves, which travel through the specimen, due to the refractive index of the specimen, while direct light waves traveling around the specimen remain unaltered. The phase contrast microscopy takes advantage of this phase difference between direct and altered light by transforming it to amplitude changes, which can be then detected by human eye or a CCD camera, for example. [**9**]

The key concept in phase contrast microscopy is the retardation of the light waves, which travel through the specimen. Retardation happens because either the refractive index or the optical density of the specimen decreases the speed of light wave when it enters into the material. After the specimen, the light wave is retarded approximately by ¼ wavelength when compared to direct unaltered light, which travels around the specimen. This phase difference is then used to create the contrast effect on the image plane. To maximize the generated contrast, the phase difference can be further increased to ½ wavelengths for the direct and retarded light waves to produce destructive interference on the image plane. This interference results in such a contrast that the image of the specimen appears dark against a bright background. [**9**]

The creation of the contrast involves the separation of the direct and the altered light from each others. This is achieved by using two light manipulating objects, which are placed in the optical path before and after the specimen. The first object, an annular ring is placed in front focal plane of the condenser. This ring passes through hollow cone of light, which is used to illuminate the specimen. Part of this light will be retarded ¼ wavelengths by the specimen, as mentioned earlier, while part of it remains unaltered. To create the final ½ wavelength retardation, this unaltered direct light is speed up by the object called phase plate. Phase plate is an objective, which has narrow and optically thinner band for the direct light. The rest of the plate is made thicker, which induces the additional ¼ wavelength retardation to the altered light, which has been already retarded by the specimen. The basic setup of the phase contrast microscope is illustrated in Figure 3.1. [**9**]

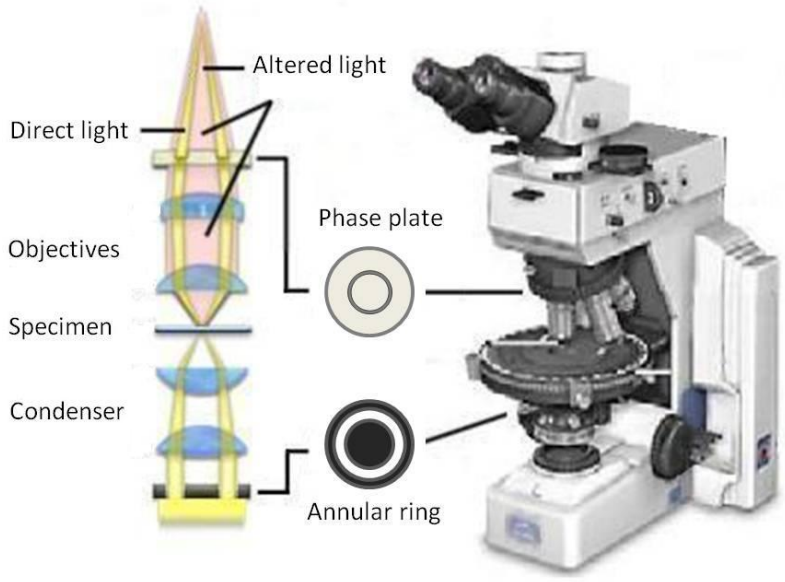

Figure 3.1. *The basic configuration of phase contrast microscope. Adapted from* [**9**]

Phase contrast microscopy provides huge advantage over standard light microscopy, without need for staining or fixing of the specimens. Especially in the case of the biological samples this is very useful, because specimens can be examined in their natural conditions. Even without staining, with phase contrast microscope it is possible to view single cells or even single cell organs. [**9**]

3.1.2. Polarized light microscopy

The polarized light microscopy is another contrast enhancing technique in the area of optical microscopy. This technique is based on the use of linearly polarized light and its modulation due to the optical phenomenon of the viewed specimen. This phenomenon is called the birefringence, which occurs when the specimen has different refractive index for light that has different direction of polarization. When birefringent specimens are observed with polarized light microscopy, the contrast is improved compared to standard light microscopy. [**10**]

Like the name of this technique suggests, the key concept is the polarization of light. Polarization is a characteristic feature for all transverse waves, and it can be applied to electromagnetic waves such as light. The electromagnetic wave is said to be transverse because the electric and magnetic fields are oriented perpendicular to each other and with the direction of wave propagation. Natural light, such as day light or light from a lamp is said to be unpolarized, because its electric field is vibrating in all possible directions. To obtain polarized light, natural light is passed through a filter, which blocks major part of the incident light by passing through only some vibration directions of the electromagnetic field. Ideal polarization filter passes through only waves, whose electric fields vibrate only in one direction parallel to the polarizing axis of the filter. Such light is called linearly or plane polarized light. Figure 3.2 illustrates this concept. [**11**]

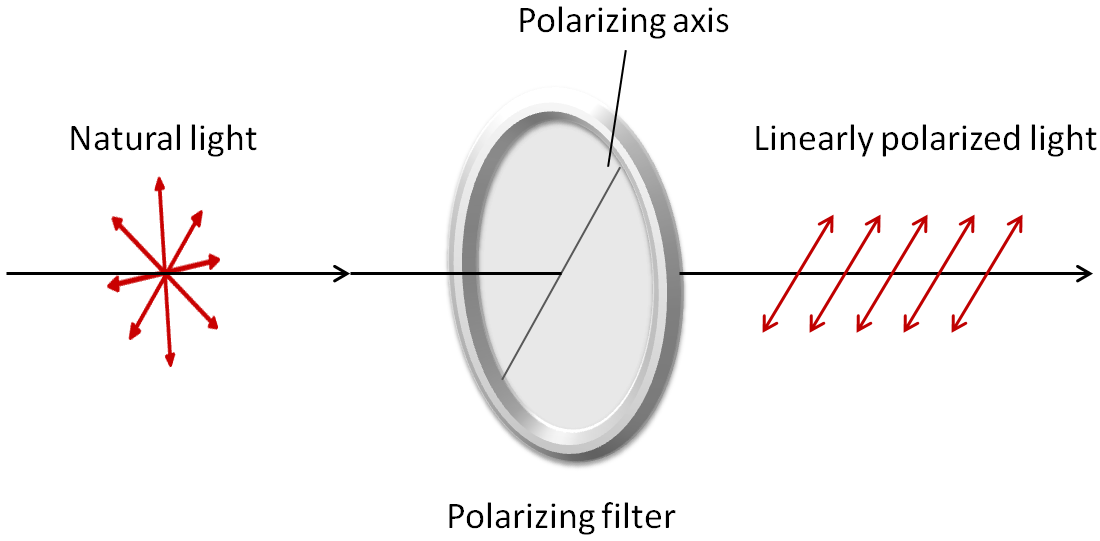

Figure 3.2. *Working principle of a linear polarizing filter. Adapted from* [**11**]

Like in the case of phase contrast microscopy, the contrast in the polarized light microscopy arises from the constructive and destructive interference between two light waves, which are out of phase compared to each other. This phase shift is produced by illuminating a birefringent specimen with linearly polarized light, which is created by placing polarizing filter in the optical path before the specimen. The birefringence, or double refraction, is a property of a material which exhibits optical anisotropy. Optical anisotropy occurs in materials, which are molecularly oriented so that the refractive index of the material is orientation dependent. The name double refraction comes from the interaction of light and the birefringent material; when light ray enters into such material, it is divided to two perpendicular components, which travel trough different optical paths having different refractive indices. One of these components, termed the ordinary ray, obeys the normal law of refraction and it has same the refractive index in every propagation direction through the material, while the other component, termed the extraordinary ray, experiences different refractive index in every direction through the material. Due to this difference in refractive indices, the ordinary and the extraordinary rays become out of phase when they exit the birefringent material. This phase shift, or retardation of the waves, is then utilized to create the resulting image contrast, which is achieved by using another polarizing filter placed after the specimen, combining the ordinary and the extraordinary rays through the constructive and destructive interference. The basic setup of polarized light microscopy is shown in Figure 3.3. [**10**]

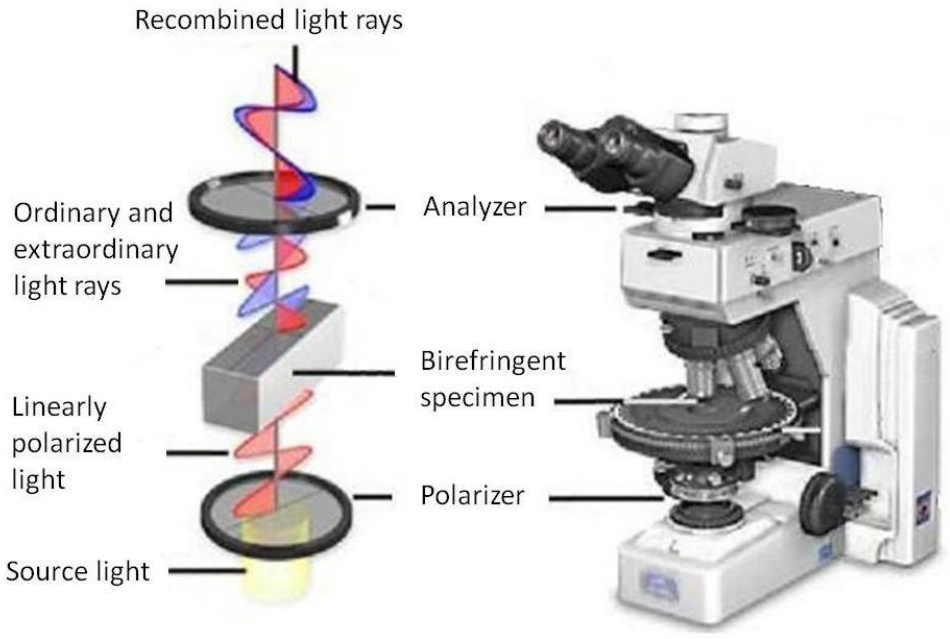

***Figure 3.3**. Basic polarized light microscopy configuration. Adapted from* [**10**]

The enhanced image contrast, when birefringent specimens are viewed, arises from the correct use of two linearly polarizing filters. After the first filter, the polarizer, electric field of the light wave has theoretically only one vibration direction, which is parallel to the polarizing axis of the filter. When this plane polarized light is filtered with the

second filter, the analyzer, intensity of the amount of light transmitted through the analyzer depends on the polarizing axis of the analyzer. If the angle between the polarizing axes of the polarizer and the analyzer is exactly 90°, and there is no specimen in the light path, theoretically all the light is blocked by the second filter [**11**]. This filter setup is called the cross polarization filter geometry, and it is most often used in polarized light microscopy. When birefringent specimens are viewed with crossed polarizing filters, only light waves that travel through the specimen, and whose polarization is altered due to the birefringence, are transmitted through the analyzer. Everything else is blocked, thus generating enhanced contrast in microscope image, where birefringent specimens appear bright in dark background. [**10**]

However, for achieving this enhanced image contrast, the polarized light microscope has to meet relatively strict requirements compared to other contrast enhancing microscopy techniques. Firstly, the linear polarizing filters limit dramatically the transmitted light intensity, thus relatively high light intensity from the light source is needed compared to other microscopy techniques. In addition, the extinction ratio, which defines the amount of light transmitted through crossed linearly polarizing filters, is maximized only in certain spectrum of light specific to the filters. Thus, the optimized polarized light microscopy requires using light of certain wavelengths to illuminate the studied specimen. Finally, the polarized light observations require special types of microscope condenser and objective lenses. Because this contrast technique is based on the birefringence property of the studied specimen which modulates the polarization state of the light, it is strictly required that the microscope lenses do not interfere in this process. Due to this, the polarization technique requires the usage of special lenses, which are manufactured by using strain and birefringence free materials. [**10**]

3.2. Digital image acquisition

Digital image acquisition plays major part of the whole data acquisition process related to this thesis. Digital image acquisition is a process, where photosensitive elements, pixels, are placed on the form of an array to collect light and to transform this information to the digital form, each pixel represented by a certain number of bits. Each pixel in this array acts as an independent light sensing element, which collects light and turns it into a charge through photoelectric effect, which is a phenomenon where electrons are emitted from material when photons are absorbed to it [**11**]. This charge is then transferred to analog-to-digital converter (ADC), which converts the voltage to a discrete binary value, corresponding to a gray level. After the conversion of the charges at all pixels, the array consists of digitized gray level values, which form the resulting digital image.

Generally all digital imaging sensors are based on the semiconductor technology, where a sensor array consisting of the photosensitive elements is manufactured from light sensitive silicon semiconductor material. Two most used digital imaging sensor

types are the CCD and the complementary metal oxide semiconductor (CMOS) sensors. Basic difference between these two technologies is that in the CMOS sensors, every pixel has its own electronics for the charge conversion, whereas in the CCD sensors the charges from all of the pixels are first transferred to a temporal register, which then sends the charge of each pixel to ADC. Because of these differences, both technologies have their strengths and weaknesses, and depending on the application and requirements, one of these technologies can be outperformed by the other. Considering this thesis work, the image data is acquired using a CCD imaging sensor, which is introduced in more details in next chapters.

3.2.1. CCD imaging sensor

In CCD architecture, every pixel is a metal oxide semiconductor (MOS) capacitor, which is used to collect the incoming light and to store and transfer the charge generated by the photoelectric effect. The MOS capacitor consists of three layers, the gate electrode, insulating layer of silicon dioxide (SiO_2) and the semiconducting substrate made of doped silicon. [**12**] The working principle of MOS capacitor is based on the potential well of the silicon substrate, which is created by applying a bias voltage to the gate electrode structure. When photon is absorbed by the silicon substrate, one electron-hole pair is generated, and the electron is collected by the potential well. The migration of negative electrons is caused by the positive voltage applied in the gate electrode. The structure of single pixel is illustrated in Figure 3.4.

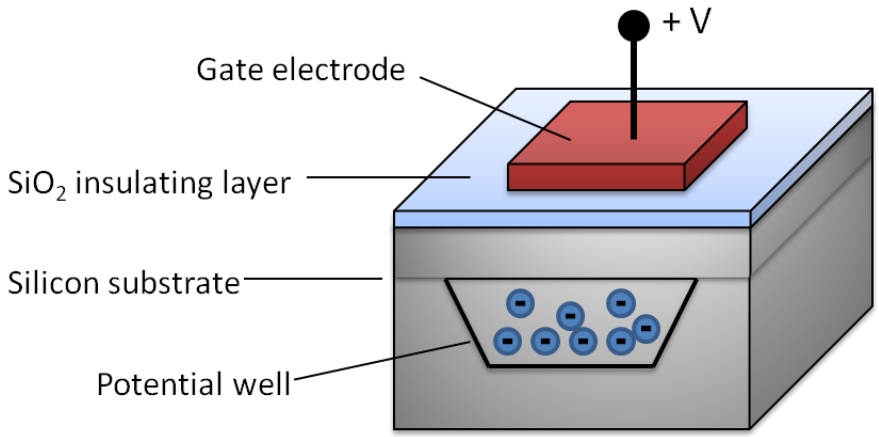

Figure 3.4. *Structure of MOS capacitor pixel. Positive gate voltage induces the potential well underneath the insulating layer, which collects the negative charge carrier electrons. Adapted from* [**13**]

The generation of the digital image is based on the ability of a MOS pixel to collect, store and transfer the charges within the CCD array structure. A sensor pixel is read out after the exposure period, during which the electrons have accumulated in the potential well. The readout process is initiated through manipulating the bias voltages of the pixel

gate electrodes in such a way that the charges from one row of pixels are transferred to the next row, and finally towards a temporary serial register located at the end of the CCD array. The actual readout process of the image is done when the serial register transfers each row of the charges, pixel by pixel to the on-chip amplifier and from there to the ADC, which converts the charges to discrete gray level values, thus forming the digital image. The readout process of the CCD array is illustrated in figure 3.5. [**12**]

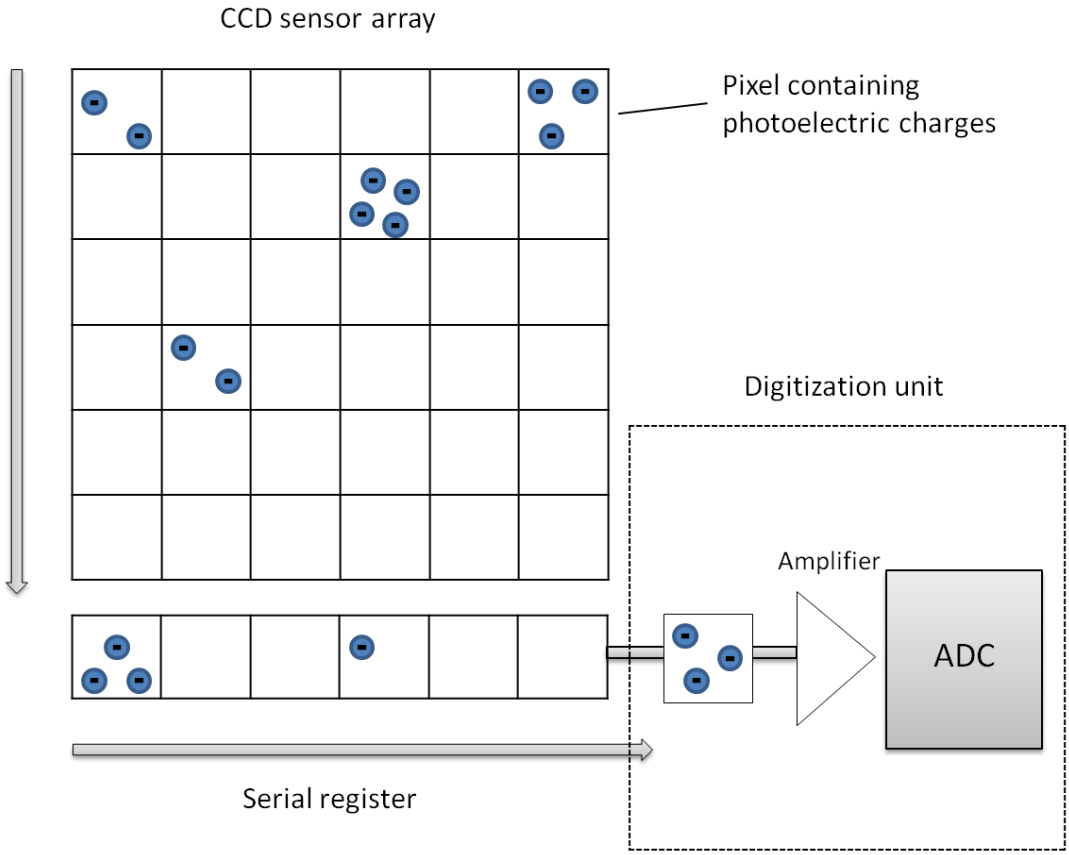

Figure 3.5. *CCD array readout scheme. Each row of pixels at a time is first transferred to the serial register, which then transfers collected charges from the row pixel by pixel to the digitization unit. The vertical arrow indicates the shift of the rows of the pixels towards the serial register, and the horizontal arrow indicates the shift of the pixels to the digitization unit.*

3.2.2. Parameters and performance of CCD imaging sensor

The quality of digital images and CCD sensors are usually defined by parameters, which characterize the resulting images and the functioning of the CCD sensor. Such parameters as temporal and spatial resolution, dynamic range, sensitivity and noise are important factors, which need to be taken into account and dealt with, if the quality of the images needs to be optimized. In live cell imaging experiments, like the ones related to this thesis, the quality of the images is usually compromised due to the requirements of high priority for some other imaging parameter settings. For example, if fast frame rate

is needed, this typically results in higher image noise originating from the readout electronics. However, the image quality in live cell imaging is crucial, because the acquired images are the source of quantitative or qualitative information. Thus the image quality needs to be optimized, for which knowledge of the imaging parameters is needed. Next, basic concepts of digital imaging sensor parameters and their relation to the performance of the CCD sensor are discussed. [**13**]

Dynamic range and sensitivity

Dynamic range is a measure, which describes the ability of a sensor to detect the dimmest and brightest pixel in an image, so that those pixels do not belong to the noise contribution. The dynamic range is defined as the ratio of the pixel full well capacity to the detection limit of the sensor, which is related to the noise contributing to the image formation process. The detection limit is defined as the lowest signal value that can be detected over the noise floor, and the pixel full well capacity defines the maximum amount of photoelectrons that the potential well of a single pixel can collect and store. The dynamic range is important measure also because it sets the requirements for the digitization unit. This requirement is the bit depth that is needed to take the advantage of the whole dynamic range, and thus to optimize the quality of the images. For example, if the dynamic range of the sensor is 4000:1, which means that sensor can discriminate between 4000 different gray values, the ADC should utilize at least 12 bits (which yields 4096 different gray levels) in the digitization process to take the full advantage of this dynamic range.

The sensitivity of the CCD sensor is defined as the amount of photoelectrons that determine one gray level in the sensor output. In the case of the CCD sensor, this setting is called CCD gain. For example, if CCD gain is assigned so that ten photoelectrons define one gray level, then 40960 photoelectrons are needed to achieve the highest gray level in the ADC unit, which utilizes 12-bit digitization depth. However, by using higher gain settings, which assigns five photoelectrons per one gray level, only 20480 (half of 40960) photoelectrons are needed to cover the whole dynamic range. Thus by controlling the gain settings, the sensitivity of the CCD sensor can be controlled. However, by using very high gains, the noise originating from the readout electronics can lead to the digitization errors, and eventually the dynamic range is compromised. [**13**]

Resolution

Other usual parameters that characterize the imaging procedure are the spatial and temporal resolution of the CCD imaging sensor. Spatial resolution tells how small details of the viewed specimen can be seen from the image, without the pixels being visible. Thus, the spatial resolution is closely linked to physical size of the pixels; the smaller the pixels, the better the resolution. Spatial resolution is also related to the number of pixels in the CCD sensor onto which the image of the specimen is projected. The resolution of imaging system has also temporal dimension. Temporal resolution, that is the frame rate

of the CCD sensor, is usually an important criterion in live cell measurements, and is one of the most important criteria considering the work presented in this thesis, because the goal is to capture electrophysiological events occurring within very short time courses. If better temporal resolution is the requirement, it usually means a tradeoff with the spatial resolution. [**13**]

Increased frame rate in the CCD architecture is achieved by either speeding up the vertical and horizontal shift speeds or applying modified sensor readout modes. The vertical and horizontal shifts, which are illustrated in Figure 3.5, define the pixel shifts towards to the serial register and from there to the ADC unit. By speeding up these events the frame rate can be hugely improved. However this method always increases the read noise, which is the larger the faster the pixels are being shifted. Considering the noise contribution, better tactic is to apply modified sensor readout modes, while keeping the pixel shift speeds as low as possible.

The simplest way to increase the frame rate is to reduce the size of the image area, i.e., to use cropping, by reading out only a sub-region from the entire sensor area. Due to cropping, CCD sensor needs to digitize smaller amount of pixels compared to full resolution, and the frame rate is increased. Another primary trick which is done to improve the frame rate is known as binning. The binning operation takes advantage of the architecture and the working principle of the CCD sensor readout operation. The binning operation combines signals from the adjacent pixels to form only a single pixel, often called superpixel, which is then read out from the readout register. Because the number of pixels which need to be read out is reduced, the number of shifts from the readout register to the digitization unit is also reduced. This allows increasing the readout rate and thus the overall frame rate, if other parameters are not changed. For example binning with factor 2x2, which means that two pixels horizontally and two pixels vertically are combined, and the readout rate is approximately twice as fast as without binning, because the rows of binned pixels need to be read out to the readout register only after every two vertical shifts. Figure 3.6 illustrates 2x2 binning readout process compared with the original readout process. [**14**]

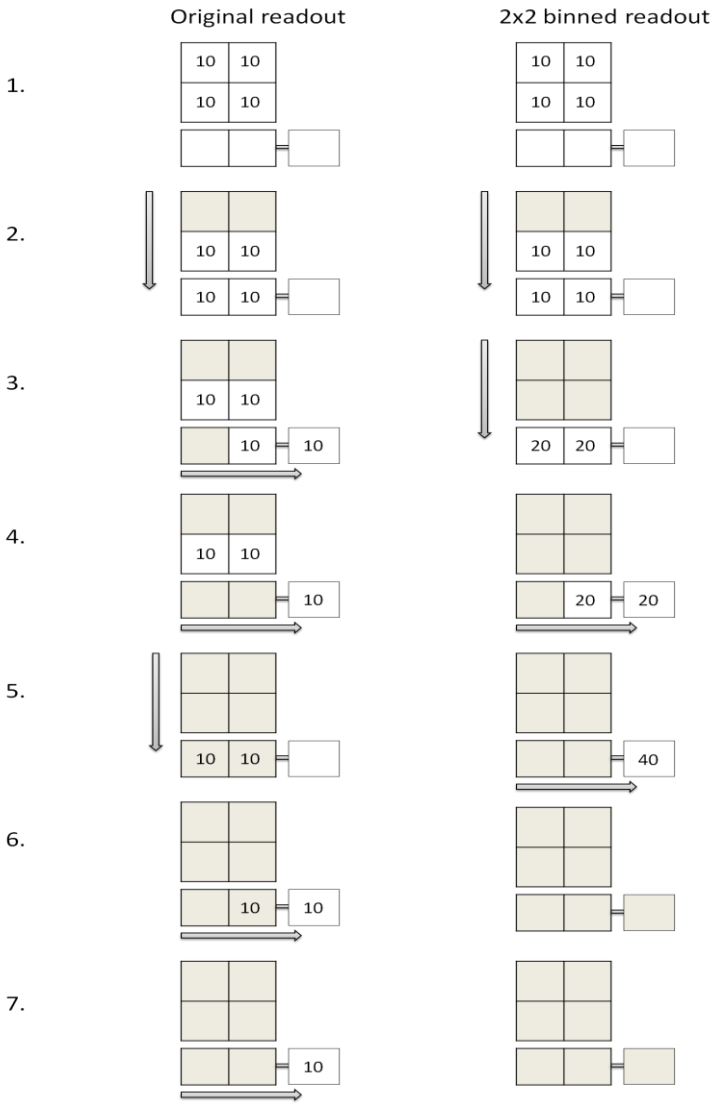

Figure 3.6. *CCD array readout in 2×2 binned mode (right) compared with the original readout mode without binning (left). Adapted from* [**14**]

From Figure 3.6 it can be seen how processing steps are reduced by applying binning mode, compared to the original readout mode. In addition, the binning operation also reduces the noise in the images, because the readout operation, which always adds the sensor originated readout noise, is done fewer times. For example, when using binning factor 2×2, the signal from the four pixels are combined and the resulting superpixel is readout only once. Thus, if we assume that those four pixels carry signal of 10 electrons and readout noise per pixel is 5 electrons, then summing up the four pixels results in the signal of 40 electrons, whereas the readout noise is added only once during the readout of this one superpixel. This leads to 8:1 signal to noise ratio (SNR) per pixel, whereas without binning the SNR would be 2:1 per pixel. Thus using 2x2 binning yields four times better SNR. [**14**]

Noise

The noise discussed so far in this chapter has been the readout noise. Consideration of the noise is important, because the noise sets the limit for the sensitivity and performance of the CCD sensor, and defines the SNR of the system.

In a digital imaging system, there are basically three types of noise sources; the photon shot noise, dark current noise and the readout noise. The dark current noise originates from the generation of thermal electrons, and the readout noise originates from the sensor electronics. These noise sources originate from the sensor itself and they can be reduced by proper sensor design. The photon shot noise on the contrary, is noise which originates from the electromagnetic radiation itself due to random variation in photon flux. Standard statistics states that the photon shot noise is defined as the square root of the measured signal, which in this case is defined as the number of measured photons. The overall SNR can be calculated as follows [**13**]:

$$SNR = \frac{Signal}{\sqrt{(readout\ noise^2 + \ dark\ current\ noise^2 + \ photon\ shot\ noise^2\ )}}$$

$$(photon\ shot\ noise = \frac{Signal}{\sqrt{Signal}} = \sqrt{Signal}\ )$$

Thus, if we assume an ideal CCD sensor (e.g. the only noise source is the photon shot noise), its maximum SNR would be shot noise limited. For example, if the measured signal is 100 electrons, then the theoretical maximum SNR would be 10. In practice there is no such ideal sensor, and the total noise is defined as the sum of all three noise sources. However, the dark current noise can be effectively reduced by lowering the temperature of the sensor. By lowering the temperature to -30ºC makes the dark current noise negligible, and professional scientific CCD sensors can be cooled near to temperature of -100 ºC [**13**]. In addition, in live cell measurements, the light intensities measured are usually very low, which means that the photon shot noise is also relatively small. Thus the only effective noise source is the readout noise, which in practice sets the detection limit and the sensitivity of the sensor in low light conditions. This noise source can be reduced by modifying the sensor readout process, like by using the earlier described binning process. Generally, the readout noise increases, as the readout speed increases, and this fact needs to be taken into account when a high frame rate is needed. [**13**]

3.3. Recording of electrophysiological activity

As discussed in chapter 2, the ability of the nervous system to send and process information is based on the electrochemical signaling between its main building blocks, the neurons. For understanding better how this system works, the functioning of neurons can be measured due to the electrical nature of the action potential mechanism. Basically, measuring the electrical activity of a neuron is a very simple process, which involves placing an electrode on or through the cell membrane of the neuron, and measuring the

changing electrical potential across the membrane due to the ion flows during the action potential. One such technique is patch clamping, which has been widely used to study and measure accurately the properties of ion channels of single neurons as well as other cells exhibiting electrical activity [**15**].

However, a technique like patch clamping has certain limitations. Especially problematic are situations when there is a need for relatively high measurement resolution in both spatial and temporal domain, such as in the case of neuronal networks. Neuronal networks consist of functional connections between single neurons, and the spatial relationships of these connections play an important role in the functionality of the neuronal network. By using patch clamp technique for example, it is not possible, or at least very difficult and unpractical to measure simultaneously how a large group of neurons works in a concert. However, by using a recently developed electrical measuring method, MEA, it is to some extent possible to overcome the problem of missing spatial dimension. Although in comparison with patch clamp, spatial resolution is sacrificed, since whereas single cells are measured with patch clamp, MEA measures fields potentials generated, in general, by populations of neurons. The MEA technique, which is used in measurements related to this thesis, is discussed in next chapter.

3.3.1. Microelectrode array

The MEA technique is a special measurement technique, which has been developed especially for the purpose of combining both the spatial and temporal measurement domains. As the name microelectrode array suggests, MEA is a platform where the measuring microelectrodes are mounted in the form of an array for the purpose of measuring electrical activity from several spatial locations. In practice, MEA is coated with proper substrates, which allow biological tissues, like neurons, to attach, grow and develop to functional spatial structures. Cells are plated in MEA dishes, and a culture can remain in a single dish for a prolonged time, usually for the whole culturing period. [**6**]

Typically MEA dishes are fabricated from transparent glass so that visual inspection with a microscope is possible during the measurements. In addition to the MEA dishes, a complete measurement system includes an electronic device for signal amplification, computer software for processing and logging the measurement data, and an auxiliary heater and possibly an electrical stimulus generator. [**6**] In Figure 3.7 is shown a typical MEA dish manufactured by Multi Channel Systems MSC GmbH (Reutlingen, Germany).

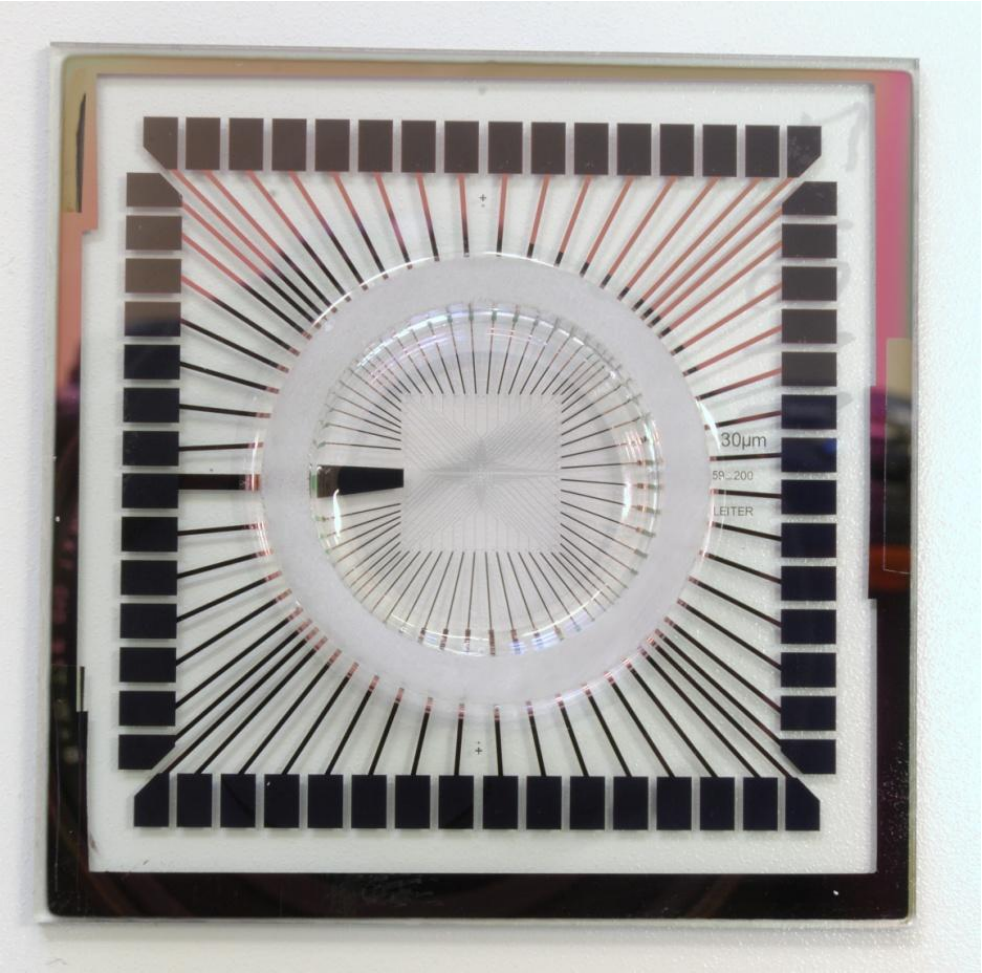

Figure 3.7. *Typical MEA dish. The microelectrode area is located in the middle of the dish, and the large electrode to left of the array acts and the ground and reference electrode.*

Although the working principle of the MEA is to perform relatively simple extracellular recordings from the cells in the vicinity of the microelectrodes, the concept of using several measuring microelectrodes simultaneously, offers possibility to measure spatial information from the studied specimen. MEA technique also enables long-term monitoring of cell cultures, because there is no need to move the specimens from the MEA dishes during the measurements and culturing, given that the environment in the MEA dishes is maintained favorable for the neuronal wellbeing. Also, the MEA measurement itself does not affect the cells. This allows the studied specimen to grow and develop into functional spatial structures during the maturation of the specimen, which provides important knowledge about the properties of naturally developing neuronal networks, for example. In addition, the MEA technique provides the possibility to stimulate the examined specimens with current or voltage pulses. Like in the case of neuronal networks, stimulation can be used to study the activity of the network in response to the given stimuli, which is important in pharmaceutical experiments and other experimental research. [**6**]

Even though the coarse spatial resolution is the major benefit of the MEA technique, it is the origin of some drawbacks too. Depending on the size of MEA electrode, whose diameter is between 10 and 100 µm, one electrode measures the electrical activity of several cells simultaneously, because the electrodes are often located under relatively dense cell layers. The problem is thereafter the fact that the electrical signaling from individual cells cannot be separated, and the actual number of cells contributing to the measured signals is not known. This drawback renders the overall spatial resolution of the MEA system more or less limited compared with that of microscope imaging or patch clamp method. Some compromises can be made by varying the sizes of the electrodes and the interelectrode distances to get better spatial resolution, but decreasing the electrode size comes with the price of increased measurement noise, which is an important factor affecting the reliability of the measurements in the sense of detecting events with relatively small signal amplitudes. It is always a trade-off between the size of an electrode and the noise: by using larger electrodes the noise level gets smaller but then the spatial resolution is decreased, and vice versa. [**6**]

4. DYNAMIC IMAGING OF FAST INTRINSIC OPTICAL SIGNALS

This chapter is one of the most important chapters in this thesis, because it introduces the backgrounds and theories related to the neuroimaging method, which is to be developed in this thesis. The chapter is divided to two parts: the first part covers the mechanisms inducing the optical signals in the neuronal tissue based on the literature, and the second part discusses the detection of these signals by using a high resolution CCD imaging sensor. The first part goes relatively deep in to the theory, but it is essential knowledge to be able to understand the mechanisms underlying the optical phenomena, and especially for optimizing the detection system.

4.1. Concept

The purpose of the dynamic imaging of FIOS is to reveal spatial and temporal information about ongoing electrical activity in neuronal tissues and cells. This imaging method is based on the changes in the optical properties of the specimen due to action potentials, which results in observable changes in the intensity of the light transmitted through the specimen. These optical signals, FIOS, provide functional information about neuronal activity partially similar to that of voltage sensitive fluorescent dyes for example, which provide information also directly on the changing membrane voltage. Whereas FIOS cannot provide information on the membrane voltage, nevertheless, similar information on the existence of the action potentials should be obtainable with both methods. The fluorescent dyes, which are nowadays widely used in neuroscience provide valuable and well defined information about neuronal activity with good temporal resolution, but the fact that fluorescent dyes are generally toxic or at least harmful by nature, restricts their applicability and allows them to be used only in experimental studies [**16**]. The FIOS imaging provides a highly valuable alternative, because it is based on the properties of the tissues themselves in the purely non-toxic and natural environment. Therefore, this imaging method could be used in both experimental and clinical studies [**17**].

The FIOS based imaging method is based on the discoveries by Hill and Keynes, who observed changes in intensity of scattered light using photodiode recordings during excitation of a crab leg nerve [**1**]. Similar results were observed later by Cohen et al. who studied the changes of axon birefringence during action potential [**18**]. The problem concerning these pioneer studies was that the signals were relatively small, and thus they needed extensive signal averaging of hundreds to thousands of single trials. How-

ever, due to the developments of imaging and microscopic techniques, the sensitivity of the imaging sensors has improved dramatically, which has enabled easier detection of FIOS even on the level of thin processes of single neurons without signal averaging. This was first demonstrated by Stepnoski et al. who observed changes in light scattering in single cultured neurons from Aplysia [**19**].

Especially nowadays, the performance and sensitivity of the CCD and CMOS imaging sensors has made the high resolution imaging of FIOS possible, thus providing high sampling resolution in both spatial and temporal domains in contrast with the former studies, which were conducted using only single photodiodes. The advantage of the dynamic high resolution imaging is that it provides a possibility to create a visual map of the functional locations and structures of the imaged tissue. In addition, because there is no need to use any kind of markers or dyes, given proper imaging equipment and image processing algorithms, high resolution imaging of FIOS is in principle a simple method compared, e.g., to voltage sensitive dye imaging.

4.2. Cell mechanisms behind dynamic optical signals

Although some research related to imaging of FIOS has taken place since the earliest studies by Hill and Keynes and Cohen et al. over 60 years ago, there is still no clear understanding of which properties of the neuronal tissue during activation contribute to the changes in the observed light intensity. However, the pioneering studies suggested that these optical signals can be separated to two categories, which differ by the optical mechanisms in the interaction between light and material, and the time needed to observe the signal changes.

The first category, observed with scattered light, corresponds to the optical signal changes having two phases. First phase is rapid optical signal change, which is coupled tightly with the rising phase of the recorded membrane potential, while the second phase follows the falling membrane potential after a varying time delay. Based on their observations, Hill and Keynes proposed that these changes would be related to the action potential induced changes in the neurons refractive index, which can occur due to the neuron volume changes or changes in the optical properties of the membrane [**1**]. Considering the second category, the studies performed by Cohen et al. showed evidence of a faster signal, which followed closely the entire action potential recorded with intracellular electrodes. This fast optical signal change, which had similar time course and shape as the action potential, was recorded using polarized light microscopy technique discussed in the section 3.1.2, which allows the observations of birefringent objects. According to these observations and the fact that birefringence is an optical property of the viewed object, the authors proposed that these observed signals were related to changes in the structure of the cell, such as reorientation of the membrane proteins, which further affects the anisotropic properties of the neuronal cell membrane [**18**].

Studies that have been conducted more recently, have continued to explore the FIOS and their origins. Although the true mechanisms behind FIOS still remain unconfirmed, there is a fairly good agreement that the main components participating in the generation of FIOS are the cellular swelling and structural changes in the cell membrane, just like the pioneering studies hypothesized. In addition, it is also frequently proposed that both of these factors contribute together in the generation of FIOS by somehow changing the refractive index, scattering of light and birefringence of the specimen [**17**]. Chapters 4.2.2 and 4.2.3 explore these cell mechanisms in more detail, but in the next chapter, basic interaction of light and neuronal tissue in the case of FIOS generation is discussed first.

4.2.1. Dynamic optical signal generation in neuronal tissue

Basically any kind of action potential related structural change, which causes variation of light propagation through the neuronal tissue, contributes to the generation of FIOS. Such optical phenomena as absorption, scattering, reflection and refraction are well known interactions between light and material, and they can all contribute to the generation of FIOS by decreasing the transmitted light through the specimen [**20**]. However, in the case of cultured neurons and neuronal networks, the absorption factor can be excluded, because those specimens lack hemodynamic functions such as blood flow and oxygenation of hemoglobin, which are major light absorption factors in functional neuronal tissue ensembles like brain [**21**]. Those hemodynamic factors have certain visible light absorption spectra and the FIOS observed in the earlier studies showed no significant wavelength dependency, which also suggests that absorption can be neglected [**1**] [**18**] [**19**]. In addition, the reflection and refraction factors are not dealt with independently, because they are summarized to scattering phenomenon in the case of biological tissue, as later discussed. Thus, when operating in the visible light spectrum, the propagation of light through single neurons and neuronal networks is simply affected by the scattering process. [**22**]

As a phenomenon, the scattering is defined to be interaction between small particles and the electric field of light, which sets electric charges in the particles to oscillatory motion [**11**]. These oscillating particles emit new light waves, whose electric fields vibrate in a plane perpendicular to the propagation direction. This is due to the transverse nature of the light wave, like discussed in chapter 3.1.2. In addition, these light waves are linearly polarized in the direction that is perpendicular to the propagation direction of the new emitted light wave. [**11**] Basically, in optically dense material, scattering particles scatter the incident light in all possible directions and the intensity of transmitted light field in some direction is the superposition of scattered fields in that direction [**22**]. The laws of interaction between light and material, and the resulting scattering, are all derived from the Maxwell´s equations, which define the complete nature of an electromagnetic wave such as light. A lot of scattering theories have been developed, which deal with the scattering under different conditions like varying size, shape,

number of scattering particles and wavelength dependency. Those theories are usually divided into two categories; single particle scattering theories such as Rayleigh and Mie scattering, and multiple particle scattering theories like Rayleigh-Gans scattering [**22**]. All of these theories require dealing with the Maxwell´s equations, and understanding of how they are developed requires deep and complex mathematics, and since that deep knowledge on scattering is not needed for this work, they are beyond the scope of this thesis.

On a macroscopic scale, scattering of light can be seen as a phenomenon where light rays change their propagation direction due to the obstacles like small particles in their path or because of the changed velocity of light rays in the material. On the other hand, such phenomena like reflection and refraction of light also alter the propagation direction of light. However, the concepts of reflection and refraction are usually defined and used in the case of smooth surfaces, where single reflection and refraction angles can be defined by the laws of reflection and refraction [**11**]. In the case of rough surfaces like biological tissues, there are no such single angles but the light is reflecting and refracting in various direction. In this case, light rays are said to be scattered, thus the reflection and refraction can be summarized to macroscopic scattering phenomenon [**23**]. Figure 4.1 illustrates the concept of light scattering in rough particles like biological cells and tissues.

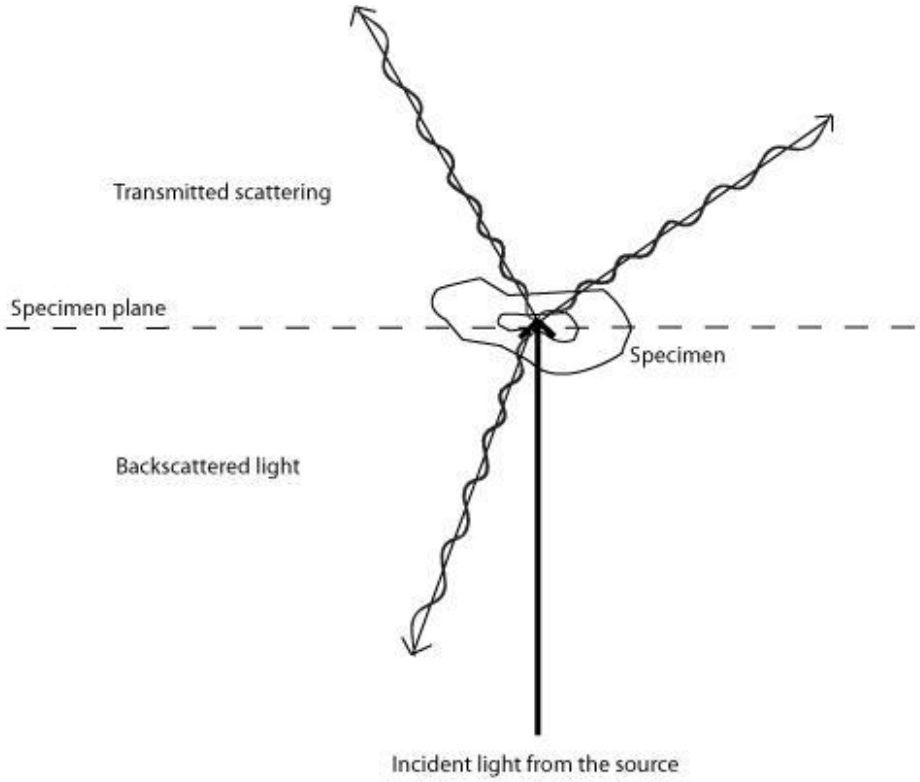

Figure 4.1. *Light scattering from biological sample.*

Considering the optical point of view, the scattering of light is dependent of the refractive index of the material where it travels. Refractive index η is defined to be the

ratio of the speed of light c in the vacuum and the speed of the light v in the material [**11**]:

$$\eta = \frac{c}{v} \quad (1)$$

Because the velocity of light in material is slower than in the vacuum, the refractive index is greater in material than in vacuum, for which the index of refraction equals to unity [**11**]. The greater the refractive index of the material, the slower is the velocity of light in that material, thus refractive index can be considered as a measure of optical density of a material. In addition, due to the wave nature of light, also the phase information of a light wave needs to be taken into account. When the velocity of a light wave changes due to the different refractive index of some material, the phase of that light wave changes as compared to a wave travelling outside the material and whose velocity does not change. Objects which introduce such phase function are called phase objects. The phase shift $\Delta\varphi$ of a light wave with wavelength λ passing through an object with diameter d and refractive index difference $\Delta\eta$ between the materials is defined as follows [**23**]:

$$\Delta\varphi = \frac{2\pi d\,\Delta\eta}{\lambda} \quad (2)$$

Biological cells, like neuronal cells, act as phase objects where the phase shift and scattering arise primarily due to relatively large change in refractive index at the boundaries of the cell membrane and the extracellular fluid, and the membrane and intracellular space filled with cytoplasm. The cell membrane structure consisting of phospholipids has mean refractive index of about 1.48, and the extracellular and intracellular space consisting of aqueous solution of ionic salts has mean refractive index of about 1.38 [**23**].

Considering the light propagation in neuronal tissue and its relation to FIOS, it is important to notice that everything is based on the changes in refractive index of the neuronal tissue during action potential. Although the refractive index, scattering and phase shift are closely linked together, the latter ones are just phenomena used to explore the variation in refractive index. In addition, scattering and phase information have been explored separately in existing studies because they have resulted in different time courses and magnitudes for the measured FIOS, which suggests that different cellular mechanisms contribute to the generation of FIOS during neuronal activation. One reason for this separation is also that scattering of light is angle dependent, and the measured FIOS in this case are variations in angular scattering. This does not take into account the phase information at all. The phase shift on the other hand can be measured with techniques that exploit the concept of constructive and destructive interference, like the polarized light microscopy, which exploits the phase shift in the form of changing birefringence of the studied specimen. Next two chapters discuss the possible cell mechanisms behind the scattering and birefringence components of FIOS.

4.2.2. Scattering component

Considering scattered light FIOS, the measured optical signals are varying light intensities that vary also as a function of a scattering angle. A study conducted by Stepnoski et al. explored the angular dependency of the scattering profile from single neuron, by measuring transmitted scattering intensities for forward angles (~0° degree) and right-angles (~90° degree). According to the results from this angular dependent scattering experiment, it was found that the measured FIOS that followed closely the membrane potential, were dependent on the measurement angle so that the amplitude and sign of the measured signals varied as a function of the scattering angle [**19**].

As an explanation for the scattering changes, the authors developed a model where dipole molecules in the membrane of the neuron reorient themselves along transmembrane electric field induced by the action potential. According to the model, the membrane dipole reorientation results in change $\Delta\eta$ in the refractive index of the membrane [**19**]:

$$\Delta\eta = \eta^n \frac{\Delta V}{d} \qquad (3)$$

In this equation η^n is the refractive index change due to the change of the membrane potential ΔV and thickness d of the membrane. According to the results where scattering changes were examined as a function of the membrane voltage, Stepnoski et al. estimated that $\eta^n = 1.2\times10^{-4}$ [**19**]. On a recent review of this theory, Kleinfeld et al. calculated the change of refractive index $\Delta\eta$ for a 1.8 nm thick membrane and 50 mV membrane voltage [**24**]. With these parameters the change of refractive index was $\Delta\eta = 3.33\times10^{-3}$ [**24**]. In addition, this change in refractive index corresponds to an average optical phase shift of about 1×10^{-4} to 2×10^{-4} radians per spike, which according to [**19**] and [**24**] could be directly detected also with phase sensitive device such as an interferometer. An interferometer discovers the phase shift by interfering two light beams, one of which passes through the specimen and while the other bypasses the specimen. In a later study Kleinfeld et al. managed to measure this optical phase shift with Mach-Zehnder laser interferometer technique [**25**]. Figure 4.2 illustrates the model of dipole molecule reorientation in an axon.

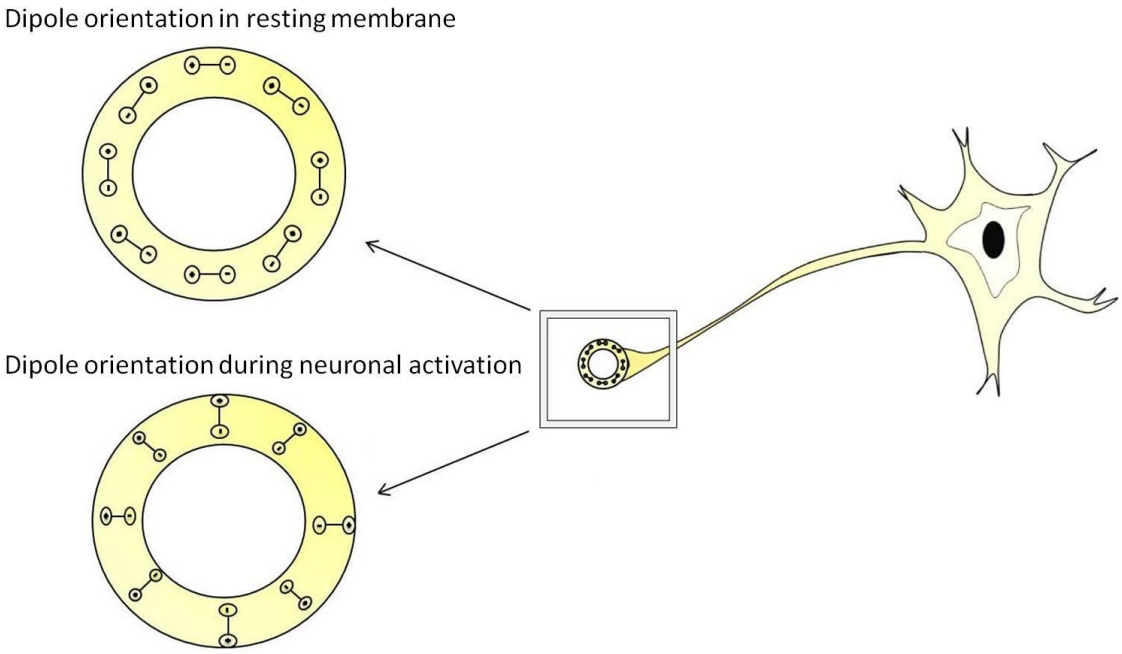

Figure 4.2. *Dipole molecule reorientation in the membrane of an axon during neuronal activation. Adapted from* [**19**]

The aforementioned model where membrane dipole molecules reorient themselves due to the changing membrane potential was already proposed in [**1**] and [**18**] and since then studies have strongly supported this model to be a possible cell mechanism behind FIOS. If such mechanism would be the only one contributing to the optical signals, then these signals should have identical time courses compared to the membrane potential during the action potential. However, since the earliest studies, FIOS measured with scattered light experiments have shown to have slightly different time courses than those of the measured membrane potentials. In fact, the optical signal changes have exhibited similar rapid rising phases as the rapid depolarizing phase of the membrane potential, but after the repolarization, the optical signal returns to the baseline after a variable time delay, i.e., the optical signal does not follow the rapid repolarization of the membrane potential. This suggests that other mechanism than just the membrane dipole reorientation affects the scattering based optical signals.

As an additional mechanism, cellular volume changes during action potential have been suggested to be a reason for delays of the scattering signal return to baseline. The action potential itself occurs due to the influx and efflux of the sodium and potassium ions, among others. It is also known that these ions are bound to the water molecules and that although most of the ions are stripped of the water while passing through the ion channels, part of the ions still remain hydrated after passing through the channels. In addition, sodium ions tend to be more hydrated than potassium ions, which lead to net swelling. [**3**] These net volume changes can contribute to the measured scattering changes by changing the diameter of neuron, which leads to changes in the scattering

geometry. In addition, volume changes are related to ion concentration changes inside the cell, and might affect the number and movements of small intracellular vesicles and neurotransmitters, which are scattering particles themselves [**26**] [**27**]. Thus, the swelling effect is proposed to be the primary reason for the delay of the scattering based FIOS, because although the membrane potential is restored after the repolarization phase, the original ion concentrations are restored by the sodium-potassium pumps, like discussed in chapter 2.1.1, which induces additional delay. It is also possible that because the sodium-potassium pumps need some time to restore the original ion concentrations, compound spike trains might induce cumulative swelling effect, which might lead to longer time delays. [**28**]

In a recent study, Rector et al. tried to separate the membrane dipole reorientation and the swelling mechanisms by measuring simultaneously both the scattered FIOS and the birefringence component of FIOS, which should arise from the modulation of the linearly polarized light due to the reorientation of the membrane dipoles, and thus follow tightly the membrane potential. Based on the hypothesis that cellular swelling contributes to the scattered FIOS, the authors used pharmacological agent manipulations which had specific effects on the cell mechanisms that control the cellular swelling [**27**]. The results from these experiments showed strong support for the hypothesis; by controlling the volume changes of the neuron with certain pharmacological agents, the delay in the scattering signal could be controlled. However, those agents did not significantly affect the measured birefringence signal. [**27**] Based on those results, authors strongly supported the contribution of the cellular swelling mechanism to the scattering signals. In addition, based on the findings, Rector et al. also preferred the measurement of birefringence signals due to the better correspondence with the membrane potential. In the next chapter, the birefringence signals and their possible origins in neuronal tissue are studied.

4.2.3. Birefringence component

As discussed earlier, birefringence is an optical property of a material, which exhibits optical anisotropy. Optical anisotropy refers to the property of the material to have different refractive index for different planes of polarization, and it is defined as the difference between the refractive index η_e for light that is polarized parallel to the optical axis of the material and the refractive index η_o for light that is polarized perpendicular to the optical axis:

$$Birefringence = \eta_e - \eta_o \qquad (4)$$

If the refractive index changes in the material where the light wave travels, phase of the light wave is retarded. This retardation in the case of birefringent material is equivalent to the phase shift $\Delta\varphi$ introduced in the equation (2), and it is defined as follows:

$$Retardation = \Delta\varphi = d(\eta_e - \eta_o) \qquad (5)$$

In this equation, d is the thickness of the material and the difference $\eta_e - \eta_o$ refers to the definition of the birefringence introduced in the equation (4).

In the case of neurons, structural birefringence occurs due to the anisotropic orientation of the membrane protein dipole molecules, like phospholipids and ion channels. In addition, the cytoskeletal components of neurons, like microtubules, exhibit birefringence [**26**]. Considering the FIOS, the optical signals measured as changes in birefringence during action potential, are strongly proposed to occur due to the conformational changes in the membrane of the neuron during action potential. This kind of conformational changes might occur because most of the membrane protein molecules, especially ion channels, appear free to rotate in the membrane and thus modulate the linearly polarized light [**26**]. According to the hypothesis, if this kind of mechanism alone is behind the optical signals when birefringence changes are measured with linearly polarized light, the optical signals should have similar temporal characteristics than the action potentials. Like discussed already in the previous chapter, the existing studies have shown that the measured birefringence changes have been strongly temporally coupled with the action potential.

A study conducted by Landowne, aimed to investigate more closely the relation of the birefringence changes and the functions of the ion channels, especially sodium channels. The sodium channel itself is a glycoprotein, which like proteins generally, is constructed of amino acids, which are bind together with peptide bonds. Landowne proposed that the conformational changes of the membrane proteins could be caused by the reorientation of those peptide bonds linking the amino acids. [**29**] Based on the results from the pioneering study by Cohen et al., Landowne presented a quantitative argument that 100-300 peptide bonds rotating 90° per ion channel could produce a change of observed magnitude in the birefringence of the membrane [**18**] [**29**]. Landowne´s calculations were also based on the knowledge that the light retardation due to the peptide bonds is proportional to their surface density, the fact that was originally explored by Cantor et al. in their studies related to biological structures [**29**].

Although Landowne´s study was focused mainly on the sodium ion channels, they noted that there are many other proteins in the membrane of neuron, such as other ion channels, ion pumps and cytoskeletal proteins, which could go through conformational changes during action potential, and thus contribute to the birefringence changes [**29**]. This is also consistent with other studies, some of which were discussed in previous chapters. Thus, the hypothesis of the reorientation of the membrane dipole molecules should be generalized to include all kinds of membrane proteins, until more precise knowledge is available. Figure 4.3 illustrates the concept of the membrane dipole reorientation and its relation to the membrane potential and the birefringence during the action potential. For comparison, the scattering signal is also illustrated in Figure 4.3.

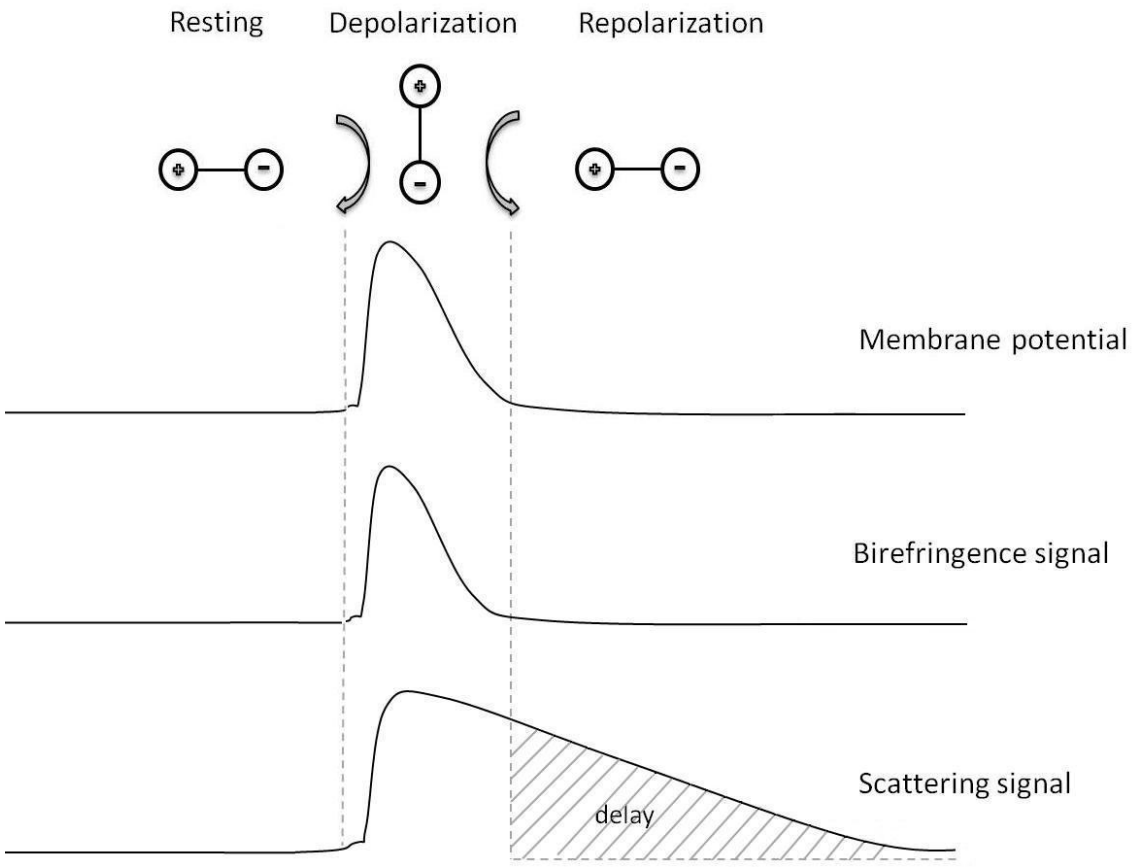

Figure 4.3. *The relationship of dipole molecule reorientation with the membrane potential, birefringence and scattering signals. The delay in the scattering signal is proposed to occur due to the alternative mechanism of the neuron volume changes, which does not significantly affect the birefringence signal.*

Figure 4.3 demonstrates both types of FIOS components, and sums up the theory introduced in the last two chapters. Although there is no absolute information about the true mechanisms behind these optical signals, the cell volume and the conformational changes are the two major mechanisms proposed in the literature. Actually, it is highly possible that these are the true mechanisms; it is just not clear if they are they acting jointly, and if so, does one component have a greater effect than the other. In fact, the joint effect was proposed in [**27**] and [**30**], which have shown the birefringence signal to exhibit also time delay as noted earlier. However, the birefringence signal delay has been significantly smaller compared to the scattering signal delay.

Although there is much controversy about the FIOS time courses, there is a clear and common understanding that the birefringence signals are much more tightly coupled with the time course of the action potential than the scattering signals. Due to this, and for the simplification of the FIOS theory introduced in this chapter, only the birefringence signals are assumed to be perfectly coupled with the membrane potential changes as shown in Figure 4.3. Although our understanding is still incomplete, the knowledge that the FIOS rising phase is always tightly coupled with the membrane de-

polarization is basically enough for the detection of action potentials. In the next chapter the dynamic optical signal acquisition and detection is discussed.

4.3. Acquisition of dynamic optical signals

Acquisition of FIOS is theoretically possible by utilizing imaging equipment, which takes advantage of the light scattering phenomena and the ability of biological tissue to act as a phase object. Maybe the simplest imaging equipment for this purpose is the ordinary light microscope. In addition to the light microscopy, a relatively new imaging technique called optical coherence tomography (OCT) has recently been used to measure FIOS. OCT is based on a similar principle as ultra-sound imaging, where coherent light from a laser source and backscattered light from a sample are combined to form a depth-resolved image. [**20**]

Most of the earlier studies were conducted using standard brightfield light microscope configuration, which was either used to measure scattered light or the phase information [**1**] [**18**] [**19**] [**26**] [**27**]. In addition, scattering signals were usually measured with varying scattering angles to explore the angle dependency of FIOS between the forward angles (~0° degree), and right-angles (~90° degree). In these studies, the optical measurements were conducted using single photodiodes to record only the transmitted light, i.e. the light from the illumination source that passes through the specimen. The magnitudes of the measured FIOS signals were different with different techniques, but usually the maximum intensity change during action potential as compared to the intensity measured in resting condition was of the order of $1\times10^{-3} – 1\times10^{-6}$. [**1**] [**18**] [**19**] [**26**] [**27**]

Although FIOS detection can be done by utilizing the basic brightfield illumination, this microscope configuration is not the most effective in FIOS detection. According to [**19**] and [**27**], the FIOS measured either with varying scattering angles or with polarization techniques have been easier to detect than using brightfield microscopy due to the better SNR of these methods. The improvements in SNR arise from the fact that huge amount of background light, which is collected with brightfield illumination, is rejected with these special microscope configurations. The background light in this case is the light that is not significantly altered due to the FIOS mechanism, and thus it can be considered as a noise in FIOS detection. In scattering FIOS measurements, the highest background light intensity occurs in the zero scattering angle (0° degree), which was shown in [**19**]. In standard brightfield microscope configuration, this zero degree background light is not rejected at all. Thus, microscope methods, which utilize only functional signals in image formation, and reject the background light not contributing to the FIOS generation, yield better SNR.

4.3.1. High resolution imaging of dynamic events

The former studies were conducted using single photodiodes to measure either scattered light or changes in sample birefringence. The advantage of using photodiodes compared to CCD sensor is the superior acquisition speed, which can easily reach sampling rates of several tens to hundreds kHz. The speed of the optical signal acquisition is highly important, because FIOS have similar temporal characteristics with the action potentials, which have time courses of the order of milliseconds. Thus, the frame rate of the optical measurement sensor should also meet these requirements. Due to the development of imaging sensors, CCD sensors can nowadays reach very high frame rates and at the same time provide highly valuable spatial information, of which the single photodiodes are not capable.

Normally, the high resolution CCD sensors do not achieve the several kHz frame rates of single photodiodes. To improve the frame rate of the CCD sensor by keeping fixed exposure time, the sensor readout time needs to be reduced, as discussed in chapter 3.2.1. For example, the fastest frame rate of our sensor using full resolution is about 30 frames/s (fps), but when the sensor is read out in a properly binned and cropped mode, frame rates from 500 fps up to a couple thousand fps should be possible according to the tests conducted by the camera manufacturer [**31**].

In the case of FIOS detection with CCD sensor, the acquisition scenario can be divided simply to two different events: the event when there is no ongoing action potential, and the event when the action potential is on. Thus, as these different events are to be detected and discriminated, single exposures of pixels should occur only during time course belonging to either one of these events. Due to this, the time course of single action potential defines the maximum exposure time that should be used to capture an event. For clarifying the concept of the exposure time and the frame rate of the sensor and how they are related to the FIOS acquisition, Figures 4.4 and 4.5 illustrate two possible acquisition scenarios.

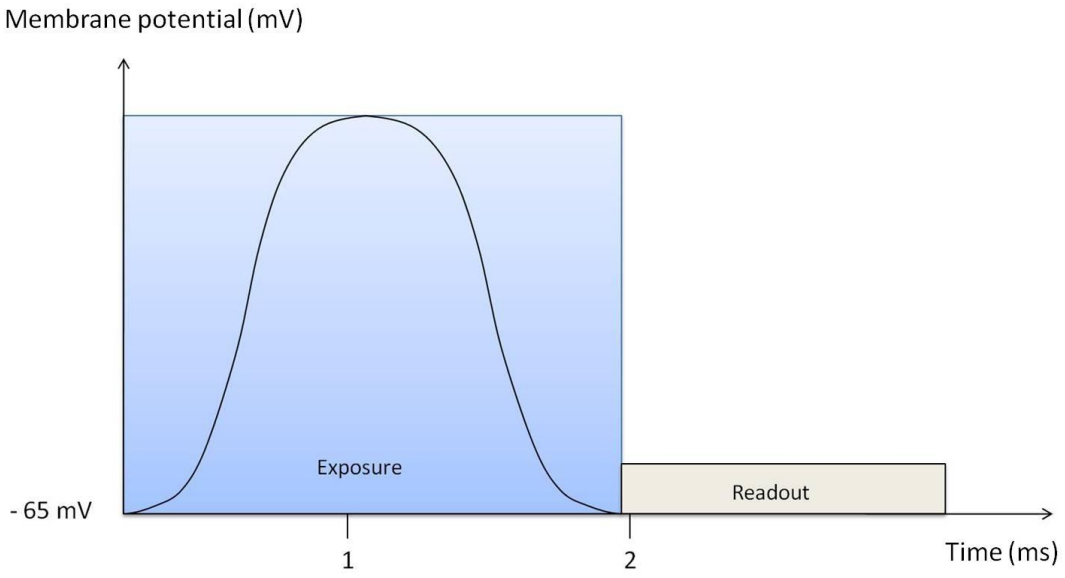

Figure 4.4. *Single exposure FIOS acquisition scenario. In this scenario only one exposure is used to cover the action potential time course.*

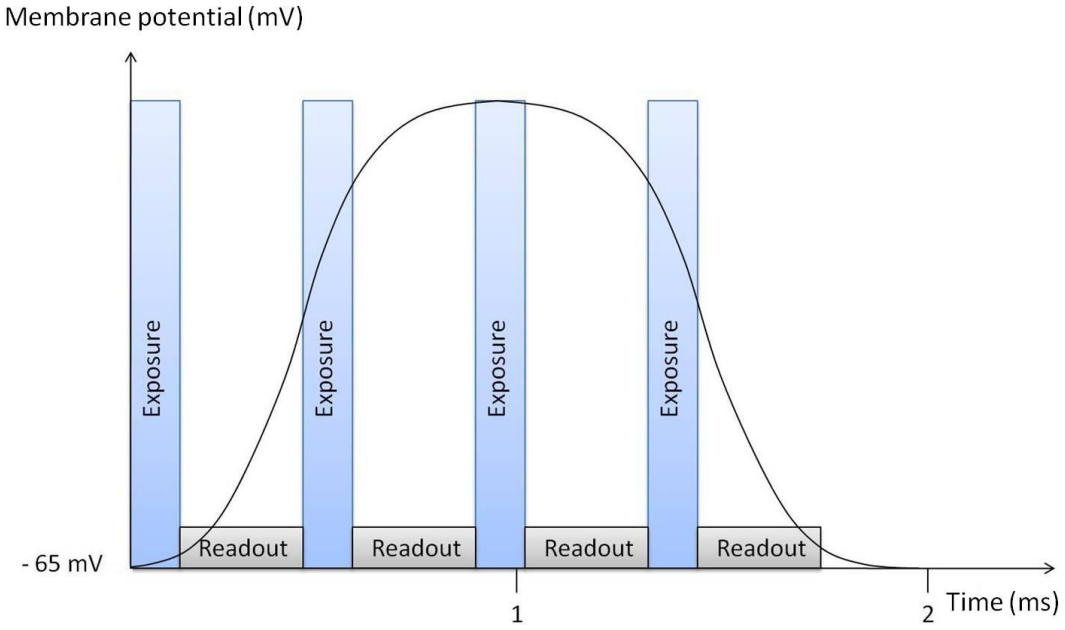

Figure 4.5. *Multiple exposure FIOS acquisition scenario. This scenario demonstrates the multiple exposures used during single action potential. Note that in this scenario the sampling time (exposure time + readout time) is much shorter and thus the frame rate much higher compared to the first scenario illustrated in Figure 4.4.*

Considering the two scenarios demonstrated in Figures 4.4 and 4.5, basically both can be applied in the FIOS detection. Considering the first case where single exposure is used, it is highly important that the timing of the exposure is synchronized so that the exposure covers only the action potential time course. However, this is practically impossible to do in the case of spontaneously spiking neurons. In addition, with single

exposure there is a possibility to get very limited information about the FIOS intensity; it gives only one value, which is the accumulated light intensity during the exposure. Only in the case when the exposure timing can be accurately triggered with the action potential, this method is reasonable to use. Even if triggering is possible, this method gives very little information about the changes in the light intensity. Although, this does not matter if the goal is just simply to detect whether there is FIOS activity or not.

The second scenario shown in Figure 4.5 is instead much more favorable in the case of spontaneously spiking neurons. By decreasing the exposure and the readout time, the increased frame rate allows to capture more samples of the changing light intensities during the action potential time course. This method does not only give more information about the intensity changes, but basically makes the exposure triggering unnecessary. This is justified because the CCD sensor can be set to continuously acquire images (image sequences), and if the action potential occurs during the capturing of the image sequence, there will be exposures, which cover parts of the action potential time course.

In this thesis, we are measuring the dynamic events of spontaneously active neurons and neuronal networks. Due to this, the better choice of the introduced exposure and sampling models would definitely be the latter one, although it requires much more from the frame rate and the performance of the CCD sensor. In addition, due to the spontaneous nature of the studied specimen, only option to capture events is to program the CCD sensor to acquire long image sequences, since cellular event could not be used to trigger imaging.

4.4. Image based detection of dynamic optical signals

After the acquisition of FIOS image sequences, detection of the dynamic intensity changes is done by using quite simple image processing procedures. Generally measurements and analysis, which are based on images, consist of basic signal processing steps, where the acquired data is usually first preprocessed. Such basic image preprocessing operations as filtering the noise and contrast enhancement, for example, can be performed to improve the quality of the images and to ease the further analyzing task. However, considering the fact that in this thesis the goal is to capture very minor signal changes that might occur at the level of single pixels, such filtering operations cannot be performed, because the dynamic signal changes would be easily detected as a noise, and would be filtered out. Thus, the preprocessing step is skipped.

The actual detection of the optical signals is done by applying a method, where one of the images from the image sequence is subtracted from the other images in that same sequence. This kind of image differencing method is familiar for example in video processing, where the changes in the scenes of consecutive frames are tracked. In the case of this thesis work, by calculating the difference between consecutive FIOS images and one reference image, the difference images should reveal the changing intensities in spatial structures that exhibit dynamic optical changes due to the neuronal activation.

The reference image, which is subtracted from the other images, can be considered background intensity. Basically this image should be acquired during the time when the neurons are not firing action potentials. This guarantees that after the image subtraction, dynamic intensity changes indicating only the neuronal activity should become observable. In this thesis, we can choose a reference image by choosing an image, which is not acquired during neuronal activity according to the MEA data.

The detection of the dynamic intensity changes can be done by applying following simple algorithm to the acquired image sequence:

(1) Choose one of the images to be the background reference image, $I_{reference}$

(2) Calculate the difference images ΔI_i, $i = 1, ..., N$, where N is the length of the image sequence, for all the images in the image sequence by $\Delta I_i = I_i - I_{reference}$.

(3) Divide all the calculated difference images by the reference image, $\Delta I_i / I_{reference}$, $i = 1, ..., N$, to obtain the dynamic fractional intensity change.

All of the operations introduced in the algorithm are done on pixel by pixel basis, which means that for example in step two of the algorithm, the difference image is calculated so that pixels of the reference image are subtracted from the corresponding pixels of the image being processed. As the result, the processed difference images reveal dynamic intensity changes in single pixel resolution. The last step of the algorithm is a kind of normalization; it is not necessary but after the operation, single pixel values shows the percentage amounts of change, which are easier to interpret compared to some arbitrary intensity values.

After the image sequence has been processed, the imaging results need to be verified. This is important especially because we are developing totally new neuroimaging method, thus we need to be sure that the results from the image analysis truly detect neuronal activity. In the case of this thesis, the ground truth information is the electrical MEA data recorded simultaneously with the imaging experiments. The image analysis is verified by comparing it with the MEA data from the electrodes, which have detected electrical activity. Because MEA electrodes record electrical activity only from their surroundings, the intensity changes in the areas close to electrodes should correlate with the electrode data.

4.4.1. Evaluation of detection performance

The performance of the introduced image based activity detection system can be evaluated with simple statistical measures. Due to the ultimate purpose of developing a method, which can simply detect the neuronal activity, the whole system can be considered as a binary classifier. In binary classification process, a system tries to classify observations to belong in one of two different categories. In this thesis, the dynamic intensity changes of the processed image pixels are the observations, which will be classified to following two categories: the category of neuronal activity and the category of neuronal inactivity.

For evaluating the performance of the classifier, knowledge of the true categories is required. In the case of this thesis, this knowledge is the information about the timestamps of electrically measured neuronal activity. These timestamps give the time points of action potentials detected in the MEA data. Because the measurements are conducted in such a way that also the timestamps of all exposures of the captured images are recorded, these two timestamps can be compared. In this case, the neuronal activity timestamps are used as a priori information in the detection (classification) process, which should detect the neuronal activity only from the images, which have timestamps matching the neuronal activity detected based on MEA data.

In binary classification process the observations are labeled either as positive or negative, thus there are four possible outcomes of the process: true positive, true negative, false positive and false negative. True positive indicates that the system has labeled the observation to be positive and the actual value is positive, and the true negative indicates the system has labeled the observation to be negative when the actual value is also negative. Thus these two outcomes are the correct ones. Other two outcomes, false positive and false negative, indicate that the system labels the observation to be either positive or negative although they are not. Thus these outcomes are the wrong ones. [**32**]

Statistical measures, which can be used to evaluate the performance of the classifier, are derived from the outcomes of the binary classification process. Maybe most used statistical measures related to the binary classification problems are sensitivity and specificity. These measures are calculated from the numbers of different outcomes, and they are defined as follows [**32**]:

$$Sensitivity = \frac{number\ of\ True\ Positives}{number\ of\ True\ Positives + number\ of\ False\ Negatives}$$

$$Specificity = \frac{number\ of\ True\ Negatives}{number\ of\ true\ Negatives + number\ of\ False\ Positives}$$

Briefly, the sensitivity describes how well the system detects the true positives, and the specificity how well the system detects the true negatives. In addition, these meas-

ures are usually applied together, because using either sensitivity or specificity measure alone, does not tell very much of the system. For example 100 % sensitivity value can be achieved by labeling all of the observations positive regardless their true condition. However, when these two measures are applied together, a better evaluation of the classifier can be done. In the case of perfect binary classifier, both the sensitivity and specificity get the value of 100 %. [**32**]

5. MATERIALS AND METHODS

This chapter covers the materials and methods for the measurements in this thesis. Both the measuring devices and the measurements themselves are described in detail. The chapter begins by first introducing the measuring environment and the devices. The end of this chapter describes the conducted measurements.

5.1. Overview of the measurement setup

The data acquisition process related to this thesis work consists of recording the spontaneous activity of neuronal cultures while simultaneously capturing digital images of the cultures. Measurement setup used in data acquisition was already built up before the measurements related to this thesis started. In addition, the setup was especially designed and built so that both the electrical and imaging data could be measured simultaneously. The core setup consisted of a MEA system, microscope and CCD imaging sensor, which were all integrated and placed inside a faraday cage on top of the anti-vibration table. Figure 5.1 shows the measurement setup.

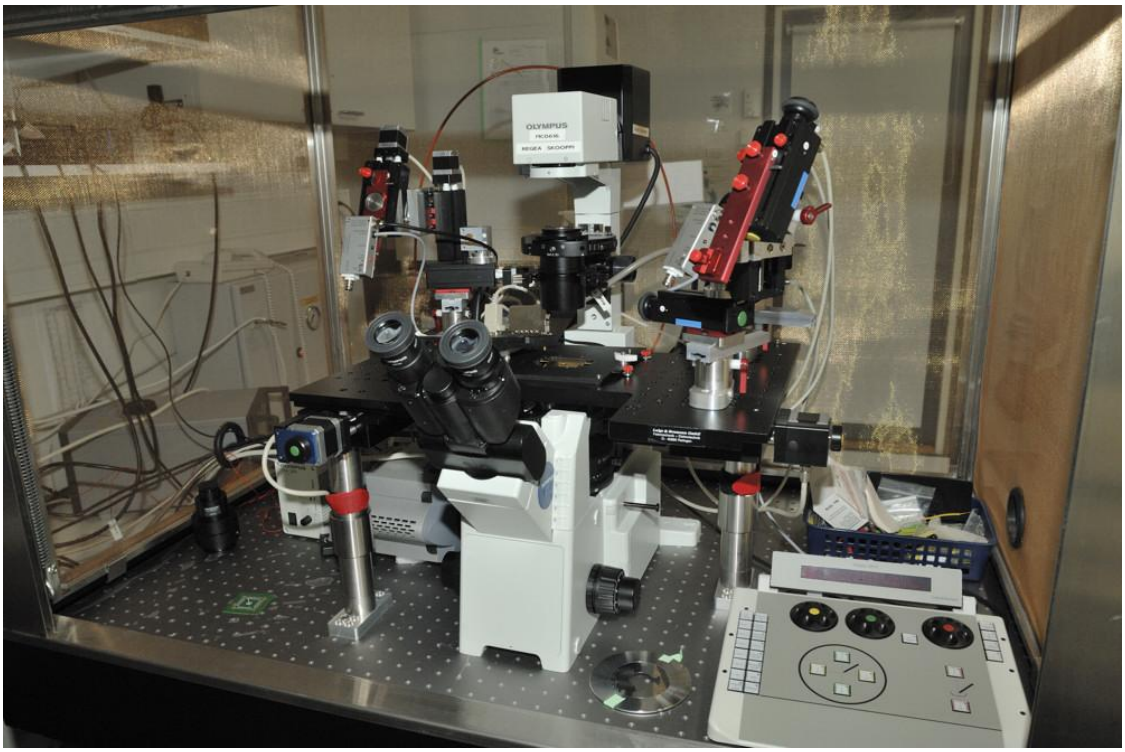

Figure 5.1. *The measurement setup. All of the core components, the microscope, MEA preamplifier and the CCD imaging sensor are placed inside the faraday cage.*

The MEA preamplifier with a MEA dish was placed on a motorized microscope table between the condenser and objectives of the microscope. The motorized table enabled fine movement of the viewed specimen under the microscope. The CCD imaging sensor was mounted on the side port of the microscope. The faraday cage around the measurement setup was installed to minimize the electrical interference. Figure 5.2 shows the measuring configuration of the setup, where the MEA dish inside the preamplifier is placed under the microscope condenser and in the optical path of the microscope.

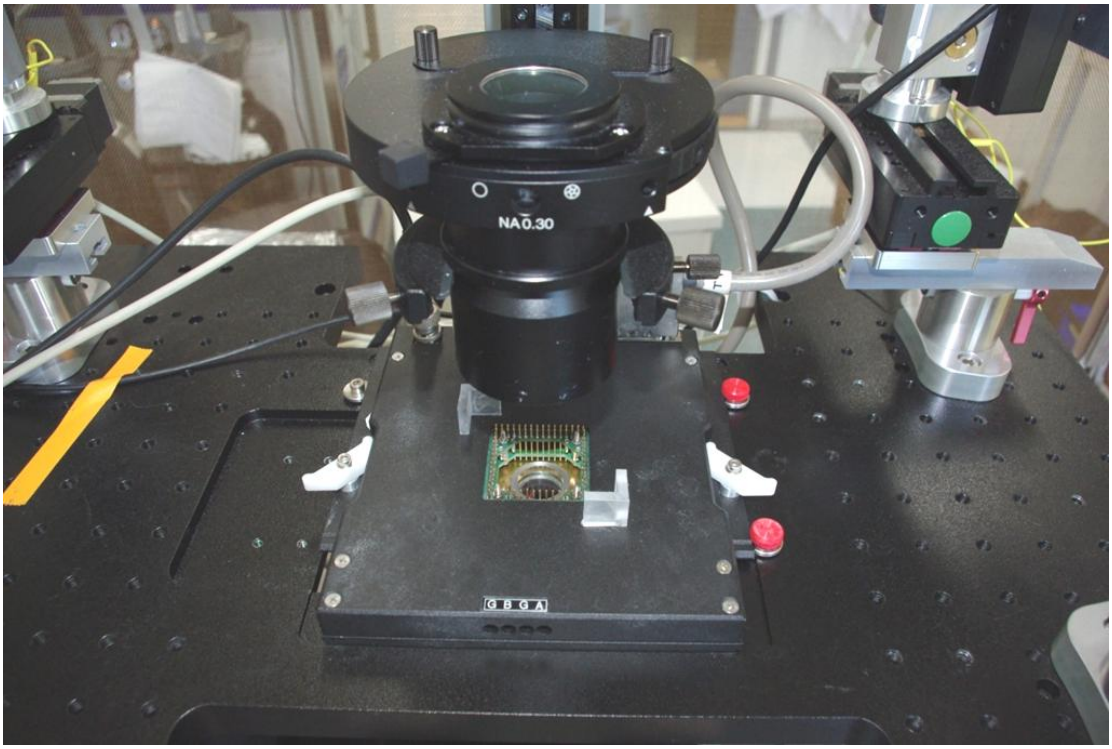

Figure 5.2. *A MEA dish and preamplifier placed in the measurement position in the microscope.*

In addition, the measurement setup included also other necessary components which are not seen on Figures 5.1 and 5.2. Both the MEA and imaging recordings were controlled by their own computers and controlling software. The MEA measurements were controlled with the MC_Rack software (Multi Channel Systems), which recorded the electrophysiological data from the MEA amplifier. In addition, the MC_Rack software was used to record microscope imaging trigger signals simultaneously with the electrophysiological data. All of the data recorded with the MC_Rack software was acquired from the digitization board located in one of the computers.

5.1.1. MEA components

The entire MEA system was manufactured by Multi Channel Systems. The main components of the setup were the preamplifier, the MEA dishes, the digitization board and the MC_RACK computer software for controlling and recording the data. The MEA preamplifier (MEA1060-Inv-BC-Standard) was designed for inverted microscopes and

the MEA system had a gain of 1100 and bandwidth from 1 Hz to 8 kHz. The measurement board sampled data with 14 bit resolution and with maximum sampling frequency of 50 kHz. The sampling frequency used in this work was 20 kHz. The MEA dishes used in the measurements were standard 60 electrode arrays (200/30iR-Ti-gr), where 59 microelectrodes measured the signal and one larger electrode acted as an internal reference and ground electrode. In this configuration the microelectrodes had the diameter of 30 µm and were spatially organized in square arrays with 200 µm of inter-electrode distance.

Additionally, the MEA setup included a temperature controller, which was used to control and maintain the temperature of the specimens in the MEA dishes at approximately 37ºC during the measurements. The setup included also a stimulus generator, which could be used to stimulate the specimen. However, the stimulus generator was not used in the measurements related to this thesis.

5.1.2. Imaging equipments

The major and most important part of the data acquisition process considering this thesis work was related to image acquisition equipments, which consisted of a light microscope and a CCD imaging sensor. In our imaging experiments, the microscope was a phase contrast microscope (IX51, Olympus). The IX51 microscope was an inverted stereomicroscope, which was optimized for phase contrast microscope observations. However, the phase contrast mode was only one illumination option, which was turned on by inserting phase plates in the optical path of the microscope. If the phase plates were not used, the IX51 microscope behaved like an ordinary brightfield microscope. In addition, the IX51 could be modified by using filters designed for different purposes, such as viewing specimens under polarized light illumination.

The CCD imaging sensor used (iXon+855, Andor) was a scientific grade, high performance sensor, which offered extreme sensitivity and full options to control the image acquisition parameters, some of which were discussed in chapter 3.2.2. By utilizing a special amplifier technique called electron multiplication, sensitivity of the camera could be tuned up so that the sensor was capable of detecting single photons over the noise floor. Other key specifications of the camera were: spatial resolution of 1004 x 1002 with pixels size of 8 x 8 µm, a frame rate of 31.4 fps with full resolution and a 14-bit of digitization depth with minimum dynamic range of 1600:1. In addition, the sensor could be cooled down to -95°C to minimize dark current noise contribution.

The image acquisition process was controlled with TILLvisION software (T.I.L.L. Photonics) in a second computer. The TILLvisION is image acquisition software, which can be used to do versatile image acquisition, analysis and image processing tasks. The software also included a standalone plug-in called the Protocol Editor, which in our measurements was used to control the camera parameters and the acquisition of fast image sequences.

5.2. Conducted measurements

The specimens measured in this thesis were hESC derived neuronal cells, which were differentiated and cultured as described in Appendix 1. Considering that the biological specimens were measured simultaneously in two different ways, the measurement routines played big role. At the beginning, it was not a straightforward task to conduct the measurements in an organized way, because relatively much effort was needed to set up the measurement devices and software to work together as desired in every measurement session. In addition, dealing with the biological samples required some additional attention and brought its own difficulties to the measurements, mainly because the environment of the cells needed to be preserved sterile all the times. However, during the work, routines became established, which not only made the measurements easier and more efficient, but more importantly, made them consistent and repeatable. These routines are described next.

At the beginning of each measurement session, the measurement setup was prepared. This prior preparation was important due to the nature of the live cell measurements, where the studied specimen needs to be measured during a relatively short time period to avoid the damage caused to the cells by the room atmosphere. In our measurements, the maximum time for which the cells were allowed to be outside an incubator, was 15 minutes. The device preparation included turning on the computers and the MC_Rack and TILLvisION software, and setting up the parameters of the CCD imaging sensor and microscope combination for fast image sequence acquisition.

Careful attention was paid to configure and optimize the microscope illumination. This step included the setting up the Köhler illumination, which is critical for achieving the uniform illumination for transmitted light microscope observations. After setting up the Köhler illumination, the type of the illumination was chosen to be brightfield, phase contrast or polarized light illumination depending on the measurement type. For the brightfield illumination, no optical obstacles were placed between the transmission light and the specimen. For phase contrast illumination, a PHC phase plate (Olympus) was inserted between the transmission light and the specimen. For the polarized light illumination, two plastic polarization filters (Edmund Optics) were placed in the light path, one before the specimen and one after the specimen. In addition, the polarization filters were placed in such a way that the polarization axes of the filters were perpendicular to each other.

The final measurement setup tuning included configuring the acquisition software of the CCD imaging sensor. Using the TILLvisION software and its Protocol Editor, the following parameters were set and used in all measurements: 1 ms exposure time, 35 MHz (maximum horizontal) readout speed and at least 2x2 binning. Other CCD sensor parameters that were configured each time, but depended on the measured specimen, were the size of the cropped sensor area and the amount of images to be captured in one sequence. A typical image sequence consisted of 1000 to 2000 images captured at 100-

150 fps. It is important to notice that these frame rates were the maximum that we achieved, however, they were much lower than desired.

The MEA dishes, which were kept in Petri dishes inside the incubator that maintained a sterile and optimum environment (temperature +37°C, 5 % carbon dioxide, 95 % air-humidified atmosphere) for the growing of the cells. After configuring the measurement devices, the MEAs were first taken from the incubator and moved to a sterile laminar flow hood. Inside the hood, the MEA dishes were removed from the Petri dishes, and a membrane that was permeable only to certain gases was attached on the MEA dishes to guarantee sterile environment for the cells also during the measurements. After these procedures, the MEA dishes were ready to be measured.

The actual measurements process was a very simple procedure. The prepared MEA dish was inserted in the MEA preamplifier to monitor and record the electrophysiological activity. One recording of the electrophysiological activity typically lasted for at least 5 minutes and at maximum 15 minutes, like previously discussed. Simultaneously with the MEA data, the MC_Rack software recorded a trigger signal for the images captured with the CCD imaging sensor during the acquiring of image sequence. However, due to the memory constrains of the image acquisition computer, the images could not be acquired continuously during the entire measurement period. The image sequence acquisition was initiated so that the electrophysiological activity was monitored in the MC_Rack software, and when neuronal activity was observed, the camera was launched to capture an image sequence. A typical image sequence lasted for from 10 to 20 s, and depending on the ongoing neuronal activity, such sequences were acquired usually one to five times during one measurement session.

After the measurements were conducted in the manner described above, the acquired data consisted of the image sequences and the electrophysiological data in such a way that the electrophysiological data files from the MC_Rack software included also the information of the image acquisition times. This linkage with the image data and the electrophysiological data was not only necessary for the analysis, but it also made it possible to reject the data that was recorded when no images were acquired, which greatly reduced the amount of the data to be analyzed.

6. RESULTS AND RELATED DISCUSSION

In this chapter, the results from the measurements are analyzed and discussed. At the beginning of the chapter, a brief overview of the measured data is given before analyzing the results. Based on the discussion of the results, the end of this chapter focuses to give propositions for the future work, which is one of the main results of this work.

6.1. Overview of the measurements and the data

Since the purpose of this thesis was to develop a novel FIOS based neuroimaging method, which involved combining the two measurement methods and joint analysis of the data, relatively much uncertainty was included in the measurement and analysis task, which affected the success of the work. In addition, to the best of my knowledge, no earlier research where single and groups of neurons had been measured using corresponding measurement equipment and procedures exist. Due to this, the requirements for the measurement equipments were not exactly known a priori, and also the outcome of the work was very uncertain.

The problems and uncertainty related to the measurements can be seen as a two-folded problem. On one side there is the measurement setup, which needed to be highly optimized due to the strict requirements of the studied biophysical phenomenon. On the other side there are the properties of the studied phenomenon and the biological specimens themselves. In the case of this thesis work, the studied specimens were spontaneous active neuronal networks. In other words, the neurons forming the network were firing action potentials randomly and basically the firing activity could not be switched on or off whenever desired. This resulted in that although the measurement equipment would have been as optimized as possible, the measurements itself were not possible, if the studied specimens did not exhibit any activity during the measurements. Also, the optimization of the measurement setup required that neuronal activity was to be measurable.

In practice, challenges appeared that were not foreseen when planning the work. The problems were related to the two categories described; the measurement setup and the measured specimens themselves. Firstly, there were a lot of problems related purely to the measurement setup not being in a prime condition. The imaging equipment, the microscope and the camera, caused serious problems, which in addition were mostly the type of problems that could not be solved, partly due to the limitations of the equipment itself and partly due to the financial and time resources allocated to this thesis work. Most seriously, it was noted that the vibration reduction table did not reduce vibration,

on the contrary, and the light source of the microscope was not stable, i.e., it flickered. The prerequisites for the successful completion of the work were that the images in an image sequence were to be aligned as perfectly as possible, and especially the lighting conditions were to be exactly the same in all the exposures. Secondly, the problems related to the measured specimens were maybe even more serious if possible; the lack of specimens exhibiting neuronal activity caused lack of applicable data. This unfortunately is always a risk with cell cultures. The small amount of active specimens, and as previously discussed, the fact that spontaneous neuronal networks cannot be switched on to exhibit neuronal activity, caused that only a very small fraction of the total imaging measurements succeeded to capture neuronal activity. Basically, the neurons and the neuronal networks could have been stimulated with the MEA system using voltage or current pulses, and thus possibly inducing the neuronal activity. However, there was no guarantee that stimulation would activate the neurons, and in our few stimulation experiments, we never succeeded to do this. In addition, the limited time that one sample was allowed to be measured per measurement day restricted the possibilities to capture spontaneous neuronal activity. Although, even if the sample had been exhibiting neuronal activity, there was no guarantee that this activity would have appeared during the relatively short measurement time of 15 minutes.

Due to the problems described, we succeeded to measure only two image sequences that exhibited the spontaneous activity of a neuronal network. Considering that we were developing a totally new method, this amount of relevant data was not sufficient. However, the results from this data and discussion about the problems related to the measurement devices, as well as the evaluation of the major error sources, are given in the following chapters.

6.1.1. Image data

The two image sequences, which were captured during spontaneous neuronal activity, were sequences of phase contrast microscope images. Although phase contrast microscopy can be basically used to detect FIOS, it is not expected to be as well applicable as brightfield or polarized light illumination based microscopy. This is because with phase contrast illumination, the FIOS information can be theoretically acquired only from the edges of the cells, where image contrast arises from the phase shift of the cell membrane and the extracellular space. Thus, there is quite limited amount of image area where FIOS can be detected. Figure 6.1 shows single unprocessed images from both of these sequences.

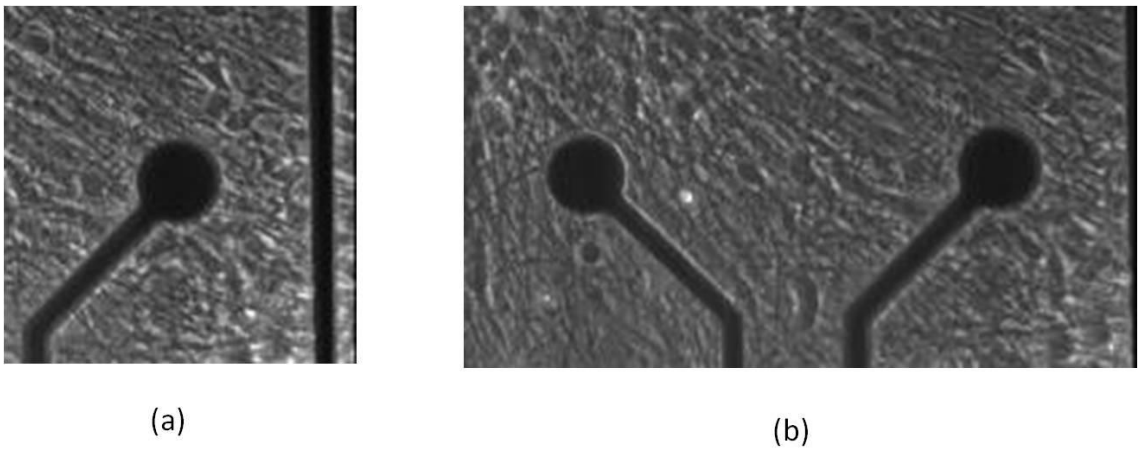

Figure 6.1. *Exemplary unprocessed images from the two image sequences to be analyzed.*

As can be seen from the Figure 6.1, contrast in the image arises only in the areas surrounding cell structures, whereas the cell structures themselves and everything else in the image contain only low and relatively even intensity values. In fact, from the phase contrast images in Figure 6.1, it is not so easy to detect single neuronal cells and their processes. This is because the network had grown a relatively dense layer of neuronal processes, and thus only some bigger structures like few neuron somas can be clearly recognized. Figure 6.2 is a magnification of Figure 6.1 (a), where a soma of a neuron is shown in a box.

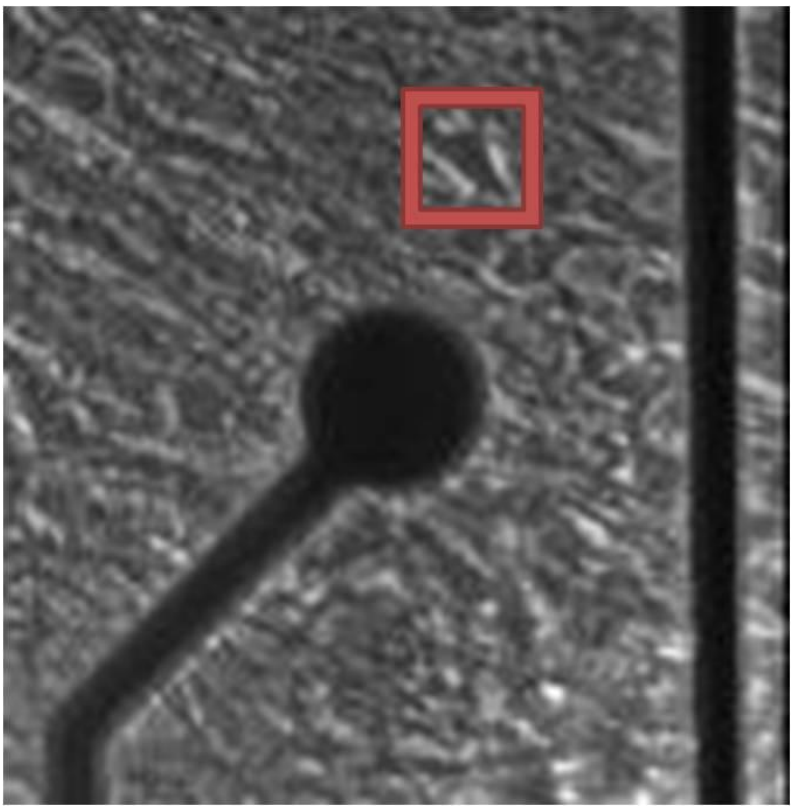

Figure 6.2. *Magnification of Figure 6.1 (a). A soma of a single neuronal cell is shown in red rectangle.*

Considering the details of these two phase contrast image sequences, they were both captured using 40x object and 4x4 sensor binning. In addition, the image area was cropped so that, the image shown in Figure 6.1 (a) contains CCD sensor area of 131×133 pixels, and the image shown in Figure 6.1 (b) covers sensor area of 251×135 pixels. By cropping to smaller sensor area, the readout time was decreased by 1 ms compared to a larger image, which yielded faster frame rate. The frame rate can be calculated from the exposure time, which was 1 ms for both images, and from the readout time, which was 6 ms for the smaller and 7 ms for the larger image. This yielded frame rate of approximately 143 fps for the image in Figure 6.1 (a), and 125 fps for the image in Figure 6.1 (b). Both of images belong to image sequences containing 1500 images, which for the faster frame rate covers the time course of approximately 10.5 seconds and 12 seconds for the slower one.

6.1.2. MEA data

The electrophysiological data recorded with the MEA system was used to verify the imaging results. Although there was a possibility to obtain a lot of information related to the specimen electrophysiology, the only information used in this thesis was the time-stamp information for the detected neuronal events, i.e., action potentials. The events detected by the MEA system are usually called spikes, whose detection is based on the abrupt changes in measured field potentials.

Briefly, the spike detection criteria related to these measurements is defined by setting a threshold value for the measured potential. If the measured potential exceeds this threshold, then the event is detected as a spike. There are different methods for defining the thresholds, but usually it is defined by calculating the standard deviation of the electrode data inside a time window. In our measurements, a moving time window was 500 ms and the threshold was set at 3.3 times the standard deviation of the signal in this window. In addition, spike detection can be triggered from the rising or falling phase of the measured potential. In our measurements, the rising phase was used.

Considering the electrical activity recorded with MEA system during the acquisition of image sequences, the electrode in the faster image sequence detected 146 spikes during the acquisition of the image sequence. In the slower sequence where the image area contains two electrodes (Figure 6.1 (b)), the electrode in the left recorded 30 spikes and the electrode in the right recorded 196 spikes during the acquisition of the image sequence.

Because we did achieve only frame rates of about 150 fps in our imaging experiments, which is far too slow compared to desired frame rates, the acquisition scenario is similar than the single exposure scenario described in chapter 4.3.1. Due to this, although the electrodes have detected spikes, there are no guarantees that all of the detected spikes have occurred during exposures of the images. The most important details of the image data as well as the electrode data is summarized in table 6.1.

Table 6.1. *Summarized details of the acquired data.*

	Sequence 1	**Sequence 2**
Images	1500	1500
Resolution (pixels)	131 x 133	251 x 135
Exposure time (ms)	1	1
Frame rate (fps)	143	125
Sequence duration (s)	10.5	12
Number of detected spikes	146	30 (left electrode) 196 (right electrode)

6.2. Data processing

A few first frames from both image sequences were chosen as background reference images, and the sequences were processed with the algorithm described in chapter 4.4.1. Figure 6.3 shows part of the processed image sequence from the Sequence 1, covering 40 images and thus the duration of 280 ms. However, for the visualization purposes only a few images including the reference image of this short sequence are shown.

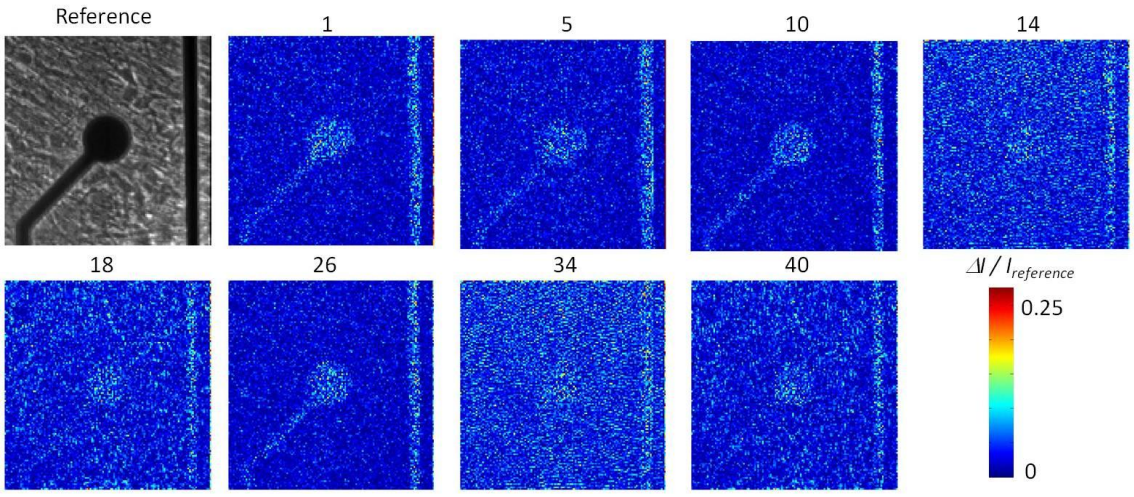

Figure 6.3. *A reference image and selected processed images from Sequence 1. The numbers above the frames refer to the frame indices. The colorbar shows the scale of the intensity change.*

From the processed image sequence, partially shown in Figure 6.3, can be seen how the intensity changes during the image sequence. Basically, there should be significant intensity changes only in the image areas of neuronal activity and in the images, which have been captured during the detected spike events. As can be seen from the images, the electrode areas seem to exhibit significant intensity changes consistently in every

image, although they should exhibit the smallest changes in those areas. However, this is only an image artifact, which arises from the normalization step in the algorithm. This is because the electrode areas contain basically only very small intensity values, because the light is not transmitted though them. Thus, even small changes in intensity can yield large fractional intensity changes after the normalization. This small intensity variation is the noise originating from the sensor digitization process, and it consists of the CCD sensor readout noise. However, this artifact is not visible, if the normalization step of the algorithm is not used.

Considering the detection of neuronal activity, we were interested in the rest of the image area, and especially in the areas covered with neuronal culture, which were chosen as region of interests (ROIs). Figure 6.4 shows mean intensity changes in one ROI, which is the image area enclosed in the red rectangle shown in Figure 6.2.

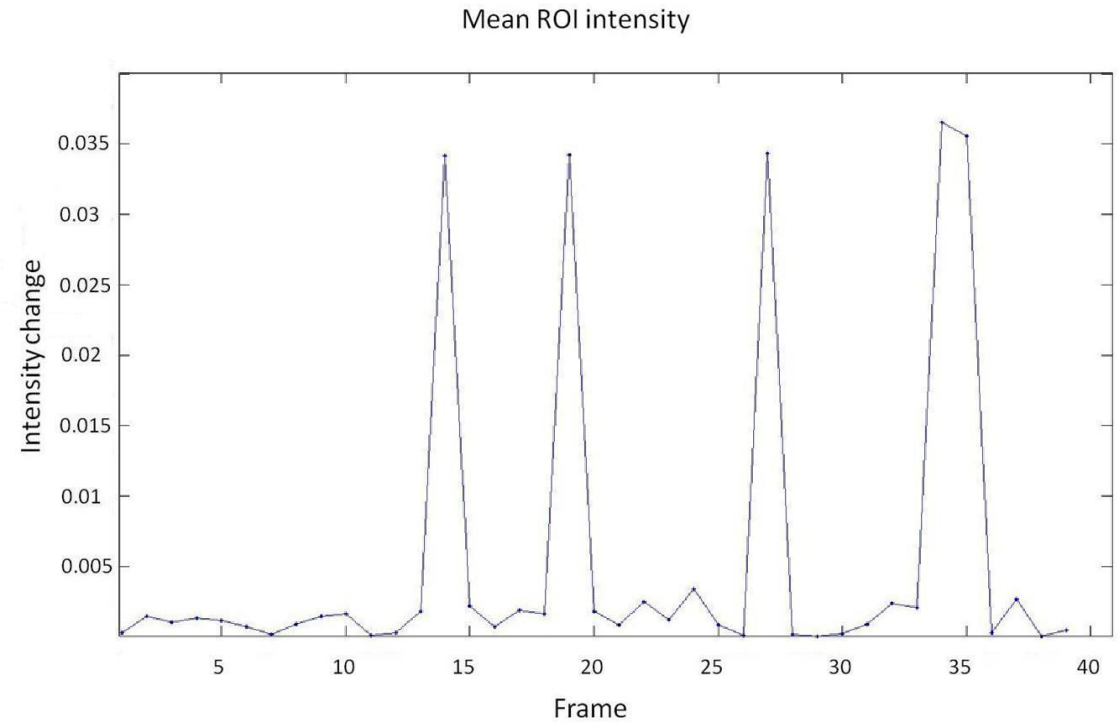

Figure 6.4. *Mean intensity diagram. Plotted points indicate the dynamic intensity change* $\Delta I / I_{reference}$. *(Data from the example sequence of 40 images, some of which are shown in Figure 6.3.)*

Figure 6.4 shows five clear peaks in the mean intensity. Without knowing anything about the recorded MEA data, it would be convenient to say that because these peaks significantly differ from the rest of the data, they clearly indicate some meaningful event occurred during the image acquisition. However, from this diagram alone it is impossible to say if those peaks truly indicate neuronal activity or not, without comparing to the MEA data.

Verification of the microscope image based activity detection is performed by first comparing the timestamps of the peak intensity images with the timestamps of the de-

tected spikes from the MEA data. Thereafter, the performance of the detection is evaluated by calculating the statistical measures of the binary classification process. For this task, the image intensity values exceeding a threshold value are labeled as detected neuronal activity (Positive), and the values lower than the threshold are labeled as detected neuronal inactivity (Negative). The threshold for the detection is defined by setting some intensity value, which clearly separates the two populations shown in Figure 6.4. The binary classification outcomes are defined as follows:

- *True Positives* are image observations, for which exposures have occurred during the detected neuronal activity, and whose intensities exceed the threshold.
- *True Negatives* are image observations, for which exposures have occurred during neuronal inactivity (no detected activity in MEA data), and whose intensities does not exceed the threshold.
- *False Positives* are image observations, for which intensities exceed the threshold although there is no detected activity in MEA data.
- *False Negatives* are image observations, for which intensities do not exceed the threshold although there is detected activity in MEA data.

Based on the numbers of different outcomes, the sensitivity and specificity measures are calculated according to their definitions, which were introduced in chapter 4.4.2.

6.2.1. Results

After processing of the both image sequences and running the evaluation of the detection performance, relatively clear results of the detection process can be stated. Before showing the full statistics, it is useful to introduce results from the short part of the processed sequence (Sequence 1), which was used as an example in last chapter. Following statistics were obtained from this short sequence, where the threshold value for the detection was visually set to be 0.01:

- Number of observations: 40
- Neuronal events detected by the system: 5
- Neuronal events detected in the MEA data: 4
- True Positives: 1, True Negatives: 32
- False Positives: 4, False Negatives: 3
- Sensitivity: 25 %
- Specificity: 89 %

From these statistics, it is still relatively difficult to make conclusions about the overall performance of the detection. This is partly because there is a relatively small amount of images (40 of total 1500), and very few spikes from the MEA data (4 of total 146), which the system should have detected. Due to this, the sensitivity and specificity measures can be largely biased. That is why the statistics of the entire sequence should be analyzed before making any final conclusions. However, some initial conclusions can be made. For making this task easier, the ROI intensity diagram in Figure 6.4 was modified by plotting the outcomes of the binary classification process and the selected threshold value in the same diagram, shown in Figure 6.5.

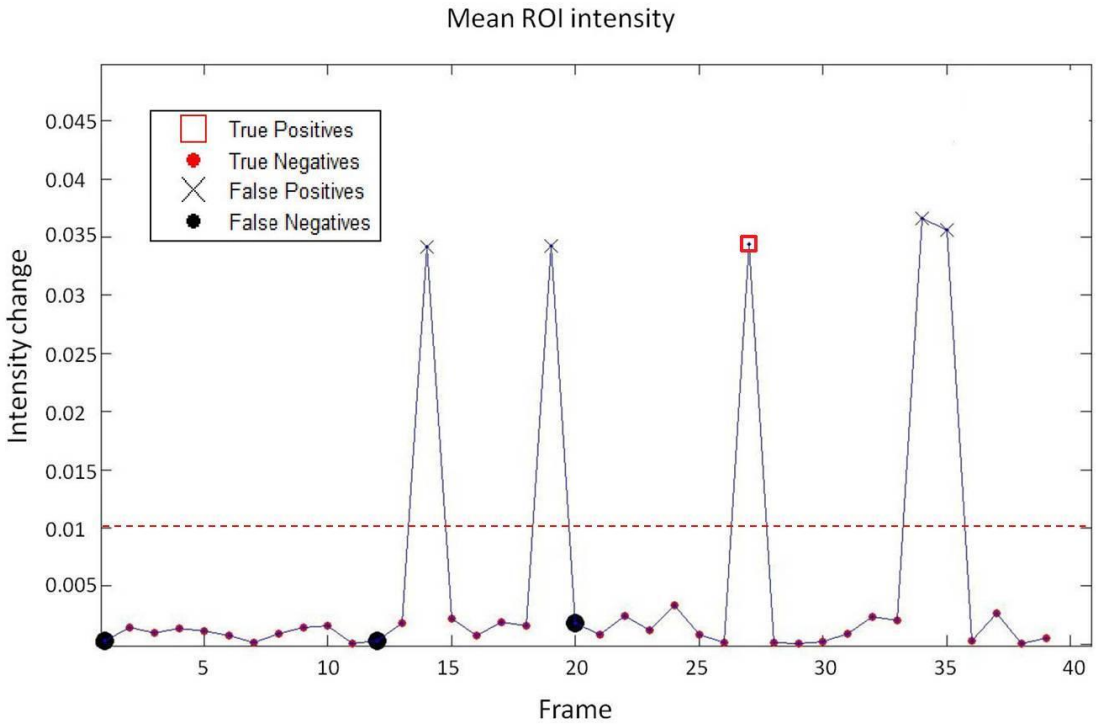

Figure 6.5. *Outcomes of the binary classification plotted over the mean intensity diagram. The detection threshold is shown with red dotted line.*

From Figure 6.5, it can be seen that the system has detected only one neuronal event correctly, which is the third large peak marked with red square in the diagram. However, the other four peaks having highly similar magnitudes are labeled as False Negatives, which means that there have not been neuronal events according to the MEA data. Because the MEA data is considered as ground truth, this strongly suggests that the one correctly detected peak is probably also only an artifact, just like the other four large peaks which were detected as False Negatives. This suggestion is also justified, because in the case of this short data part, the system has actually detected 5 events although there were only 4 true spike events according to the MEA data.

The overall performance of the detection can be evaluated by analyzing the binary classification results from the entire image sequence (Sequence 1):

- Number of observations: 1500

- Neuronal events detected by the system: 317
- Neuronal events detected in the MEA data: 146
- True Positives: 7, True Negatives: 1044
- False Positives: 310, False Negatives: 139
- Sensitivity: 4.8 %
- Specificity: 77 %

From these statistics, it is very obvious how poorly this system detects the neuronal activity. First of all, the system has actually detected 317 events although there were only 146 true events (spikes) detected in the MEA data. Thereafter, only 7 of these true events were correctly detected as True Positives by the system. In addition, the 139 observations detected as False Negatives makes the Sensitivity value as low as 4.8 %. This means that the system misses nearly 95 % of all the spikes. Although the Specificity value of 77 % is relatively high, which suggests that the system does not very easily detect neuronal activity falsely, this value is highly biased towards too a high value. This happens because there are relatively many True Negatives compared to False Positives, which ultimately is due to the far too slow frame rate of the camera.

The obvious failure of the activity detection can be explained by analyzing the ROI intensity diagrams shown in Figures 6.4 and 6.5, which reveal mean intensity dynamics from the selected ROI, which in this case was a 10×10 pixel square shaped area shown in Figure 6.2. By selecting different size of ROIs from different image areas, different diagrams should be obtained. Due to the fact that MEA electrode measures summed field potentials from its surrounding area, the entire area surrounding the electrode should taken as the corresponding ROI, because there is no more precise information about in which areas the recorded spikes were originally generated. However, when different areas and various sizes of ROIs were examined from the Sequence 1, all of the diagrams still resembled exactly the one shown in Figures 6.4 and 6.5. This was the case even when the ROI was chosen so that it covered the whole image area.

Although that this is a very confusing result, the actual reason for this is very obvious and it was actually partly known before the imaging measurements was even conducted. The ROI, which covers the whole image area, estimates the overall illumination level of the image, thus it can be directly related to the illumination profile of the transmission light of the microscope. By plotting the mean intensity of the whole image area on to the same diagram shown in Figure 6.5, it is clearly seen how the peaks, which were detected as neuronal activity, correlate with the illumination profile of the transmission light. This is shown in Figure 6.6.

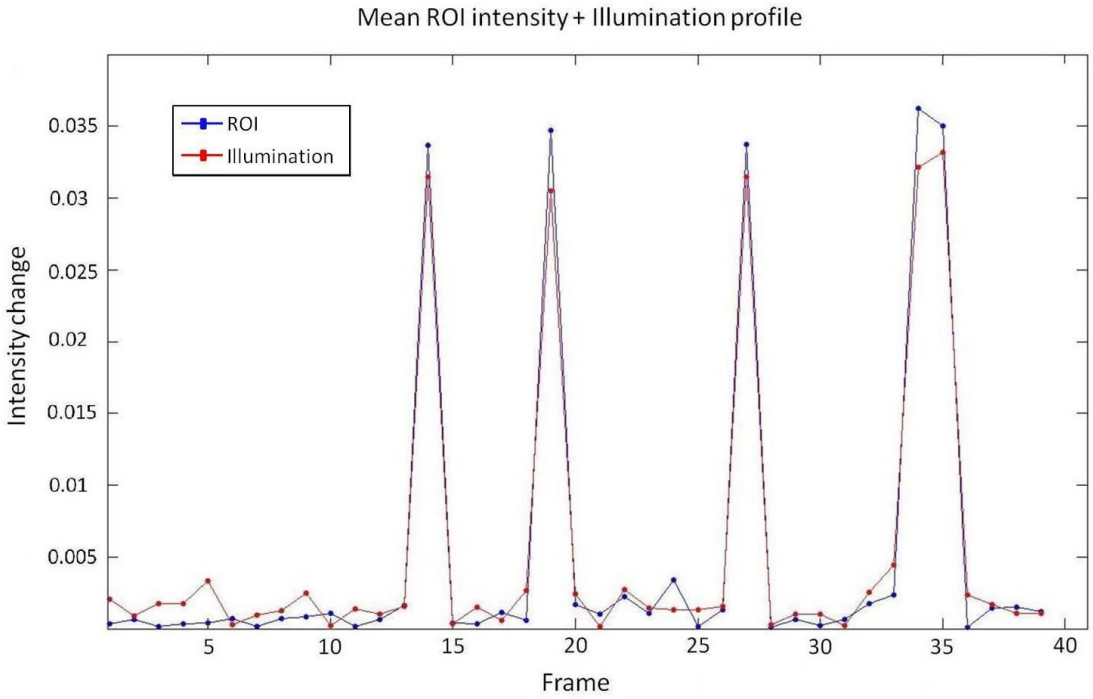

Figure 6.6. *Combined plot of ROI intensity diagram and illumination profile of the transmission light.*

From Figure 6.6, it is easy to make the conclusion that the image data is heavily corrupted due to the instability of the transmission illumination. In fact, this was the case for both image sequences (and actually for every imaging experiment conducted during the measurements related to this thesis), thus it is not necessary to analyze and introduce further the results obtained from the Sequence 2.

Considering, that the detection is done in a way, that the images in the sequences are compared to one reference image, the stability of the overall image illumination should be as good as possible throughout the entire image sequence. Although, there do not exists such optimal illumination sources which would produce perfectly constant illumination level, the magnitude of the variation in the illumination should not be larger than the detected FIOS signal magnitudes. If variation is larger, the FIOS signals are masked under the varying illumination. Unfortunately this was the case in our measurements, which ultimately caused the failure of the analysis.

Additionally, due to the lack of previous research conducted with same methods and devices, there is no knowledge of how large the FIOS magnitudes can be in the case of high resolution imaging experiments conducted with single neurons or neuronal cell cultures. In the earlier research referenced in this thesis, the FIOS were measured using single photodiode elements, which simply measure all the light focused to it by the microscope. In these experiments the measured FIOS magnitudes ($\Delta I / I_{reference}$) were of the order of 1×10^{-3} - 1×10^{-6}. It may be safely assumed that single pixel FIOS signals from a CCD sensor cannot exceed those values, but actual FIOS magnitudes remain unknown before successful experiments are conducted. However, the illumination used in our

experiments varied with magnitude over the order of 1×10^{-2}, which is clearly larger than the observed FIOS magnitudes reported in the previous studies. This fact rendered the image data acquired in our measurements very unreliable and thus relatively useless.

Due to this, also further analysis about other error sources is relatively unnecessary for considering the reliability of the results of this thesis. For example, the evaluation of the binary classification performance was not very useful, although it also revealed the fact that the measurements clearly failed to detect the neuronal activity.

However, based on the results presented here, the improvements and requirements related to the image acquisition system can be proposed for conducting the experiments successfully in future. These issues are discussed in next chapter before the final conclusions of this thesis are presented in chapter 7.

6.3. Requirements and improvements for future work

As discussed in the beginning of chapter 6, the problems related to the conducted measurements can be divided to two parts: the spontaneous nature of activity of the studied specimens and the measurement devices. However, the spontaneous nature of the specimen is not related to the reasons why the measurements failed to detect the neuronal activity. Even if we would have controlled the activity of the neuronal networks, and thus been able to produce more relevant data to be analyzed, the measurement devices were in such condition that the detection task would still have been impossible.

The following discussion focuses to cover the requirements for the successful optical signal detection. Based on the theory introduced earlier in this thesis and especially the results obtained from the measurements, the requirements are divided to two parts. The first part covers the microscope related issues, which is maybe the most critical part in the whole image acquisition process. The second parts covers the requirements related to the digital imaging sensor.

6.3.1. Optical image formation

The initial requirement for the whole FIOS detection is definitely the stability of the microscope illumination, which is used in the optical image formation. Although this might sound like a very trivial issue, it was ultimately the reason why the measurements in this thesis failed. Thus, the issues and requirements considering the light sources are discussed first. Other topics discussed after this are related to the microscope optics and special techniques, which can be used to optimize the image formation and FIOS detection.

Light source

The halogen light source used in our measurements should in principle have been stable enough for the detection process, because in all of the prior studies referenced in this thesis the same type of light source was used. Most of the literature does not explicitly

report how stable the illumination should be, however it can be argued that the illumination profile should not have larger variations than is the detected dynamic optical signals, like discussed in the previous chapter. Only in one previous work the stability of their illumination source is reported; the stability was measured to have fluctuations of the order of 1×10^{-5} while the measured FIOS had magnitudes of order of 1×10^{-3} expressed as $\Delta I / I_{reference}$ [**19**]. Thus, the argument considering the requirements of light source stability is justified.

Considering the halogen light source, which emits light covering the entire visible spectrum of light, there are couple of factors which affect the stability of the illumination. First of all, because the halogen lamp emits light according to the driving voltage applied to it, there is a big difference if the driving voltage is AC or DC coupled. If DC coupling is used, images can be sampled with maximum of 50 fps, because larger frame rate would cause 50 Hz flickering noise to the images. Thus, the light source is needed to be controlled with a DC coupled power source to avoid this artifact. In our measurements, the light source was DC coupled, but it still did not provide stabile illumination. In DC coupled method, the instability of the illumination can occur due to the poor quality of the power electronics used to transform the AC to DC voltage. Although we did not measure the DC voltage profile of the power source, it is highly unlikely that this was the reason, because the power source used (Olympus TH4 - 200) is developed for the exact purpose of generating stable illumination for sophisticated microscope applications. The only reason left for the unstable illumination is the fact that during the aging of the halogen lamp, it becomes more and more unstable. Thus, it is highly probable that this was the real reason for the unstable illumination problem.

As a conclusion, the most critical requirement for the light source used in this kind of application, is the highly stable illumination profile. To achieve this, DC coupled driving voltage should be always used. In addition, when using halogen light sources, it is important that the aging of the halogen lamp is considered. Also other light sources can be used, although the halogen is the most common in optical light microscopes. For example the suitability of light emitting diodes (LEDs) should be explored, because the LED light should be as stable as the halogen light sources. In addition, the transmitted wavelengths by the LEDs can be much better controlled due to the narrow bandwidths compared to the halogen light sources.

Microscope optics and special techniques

Regardless of the microscope technique being used, the quality of the formed images depends highly on the microscope optics, the condenser and objective lenses, which form the magnified image of the specimen to be captured by the digital imaging sensor. The lens structures and how they are used to collect the light optimally in the image formation process require deep understanding of optics. Since optics is not being developed in this thesis, actual optimization of the optics is outside of the scope of this thesis. However, the basic idea in the optimization of the microscope images is that the micro-

scope objectives should collect as much light as is available during the specimen illumination.

Considering this aspect, the microscope objectives can be divided to two categories depending of the medium between the objective and the glass plate on which the specimen is attached. Usually this medium is air, but using other immersion mediums like oil or water, the refractive index can be manipulated so that more light rays emanating from the specimen after the glass plate are refracted towards the microscope objective lens. This increases the amount of light collected by the objective and a huge improvement in the image quality is achieved compared to air immersion objects. [**33**] In our measurements, one specimen sample cultured with special MEA dish allowed the use of oil immersion objective. In Appendix 2, image acquired with brightfield microscope illumination and a 40x oil immersion objective can be compared to the corresponding image acquired with a normal objective.

Considering the microscopy techniques, different methods can be used to detect the FIOS arising from the neuronal tissue during action potentials. In this thesis, the purpose was to acquire the image data using brightfield illumination, phase contrast and polarized light microscope techniques, because each of them should allow the FIOS detection by utilizing differently either the scattering or phase information of the transmitted light in the image formation process.

However, the FIOS detection can be optimized by choosing techniques, which utilize only the light that is affected by the FIOS mechanisms. Phase contrast and polarized light microscopy both utilize the phase information, which is altered due to the refractive index changes during the action potential. Of these two techniques, the phase contrast technique is not so good, because with phase contrast, the FIOS information can be obtained only from the edge areas of the cells. Thus, the polarization based technique is much more favorable and it has been used in most of the previous studies referenced in this thesis. However, the polarization technique has also some drawbacks, which are related to its strict requirements discussed earlier in chapter 3.1.2. If these requirements are not satisfied, the performance of this technique is more or less compromised, which can lead to heavily decreased image quality. In fact, this was the case considering our polarized light setup configuration. In Appendix 2, one of these polarized light microscope images is shown.

The standard brightfield illumination microscopy does not take into account the phase information; it utilizes only the information of transmitted light intensity through the specimen. Thus, this basic microscopy method allows the detection of dynamic optical signals, which are affected by the FIOS scattering mechanism. However, this method suffers from the fact that the background light originating at near zero angles from the specimen after scattering is not rejected, which significantly lowers the SNR of detected FIOS. If this small angle scattering can be rejected, the FIOS detection is hugely improved. A very simple technique called darkfield microscopy would be the solution for this. Actually this method is maybe the simplest contrast enhancing technique in the

area of optical microscopy, which is based on the idea that only light rays scattered more than certain angles is used in the image formation. This acceptance angle is defined by the condenser and objective lenses of the microscope. Even rejecting scattering angles smaller than three degrees has been shown sufficient for improved scattered FIOS detection. [**19**]

As a conclusion of the issues related to the optical microscopy techniques, a ground rule for the optimized FIOS detection is very simple: Only techniques, which utilize mainly the functional signals in the image formation and reject the background light intensity, should be employed. Although the polarized light microscopy is widely used to detect FIOS, it is relatively difficult to achieve optimized polarization observations due to its strict requirements. Much more favorable technique is the darkfield microscopy, thus, for conducting the FIOS measurements successfully in future, this microscopy technique is strongly recommended.

6.3.2. Digital image formation

After the optical image formation is dealt with properly, the digital image formation and the actual FIOS detection task are to be considered. Basically, the requirements can be simplified to be concerned with two issues: the sensitivity and frame rate of the digital imaging sensor.

Sensor frame rate

The requirements for the frame rate were thoroughly discussed in chapter 4.3.1. The basic rule considering this issue is that the exposure of single image should occur either during the action potential time course (neuronal activity) or during rest (neuronal inactivity). Although the exposure time does not directly define the frame rate of the sensor, or vice versa, by using frame rates of several thousands of fps, it is guaranteed that a number exposures coincide with action potentials.

Basically, it is possible to acquire FIOS information by using slower frame rates, but then the optimal exposure time would be the duration of the action potential, and the timing of the exposure should be accurately synchronized with the neuronal event in order to maximize the FIOS magnitude. In the case when image acquisition cannot be triggered with the neuronal activity, the probability of acquiring optimally exposed images decreases. This was the case in the measurements related to this thesis, and only a very small fraction of the action potentials detected by the MEA system occurred during image exposures.

Sensor Sensitivity

The sensitivity of the digital imaging sensor is the final, and ultimately one of the most important issues related to the detection task at hand. Even if all the other requirements considering both the optical and digital image formation were satisfied, the whole detec-

tion would ultimately fail if the sensor was not sensitive enough to detect the minor changes in the light intensities.

As discussed in the chapter 3.2.2, the sensitivity of the sensor is defined as the number of photoelectrons assigned to trigger one gray level in the output of the ADC unit of the sensor. In the case when there is no noise contribution, the highest achievable sensitivity is obtained when only one photoelectron is assigned per one gray level. However, there are no such noiseless sensors, and thus, the sensitivity is always constrained by the detection limit, which is defined by the largest noise source contributing to the image formation process. The sensitivity and detection limit are both related to the definition of the dynamic range, which describes how small intensity changes can be detected by the sensor under constant photon flow. Considering the FIOS detection task, where the FIOS magnitudes are assumed to be, for example, of the order of 1×10^{-3} ($\Delta I / I_{reference}$)(a typical value in the literature), which means that the sensor is required to be able to detect this amount of intensity change during the action potential compared to the resting intensity, the requirements for the dynamic range of the sensor can be derived. Intensity change order of 1×10^{-3} requires dynamic range of the order of 1000:1. The CCD imaging sensor used in our measurements would have fulfilled this requirement, because it provided dynamic range of about 1600:1.

It is important to notice that because the dynamic range is always affected by the detection limit and the sensitivity settings of the sensor, each of these factors should be considered with regard to the optimization of the FIOS detection. Actually, the ultimate requirements for these factors should be derived only through quantitative photon counting operation during the action potential light transmittance modulation. The literature does not report any photon counting operations. In addition there is no exact information reported about the photodiode sensitivity settings used. Due to this, the reported FIOS magnitudes should not be directly compared with each others and also not considered as the ultimate requirements for the sensor performance.

However, because in the previous works it has been shown possible to measure FIOS, the results reported and discussions presented in this thesis are highly encouraging and potentially very useful for developing this novel high resolution neuroimaging method in future.

7. CONCLUSIONS AND DISCUSSION

The purpose of this thesis was to develop a novel high resolution neuroimaging method, which was to allow detection of neuronal activity in *in vitro* neuronal tissue samples by observing dynamic action potential related FIOS events. This development task was based on the digital microscopic imaging measurements, which were conducted after studying the theoretical backgrounds related to the FIOS mechanisms, and the methods which can be used to detect these functional dynamic signals. The theory and the measurement principles used in this work were based on the literature related to the topic.

The FIOS events, which were first discovered over 60 years ago, are minor changes in the intensity of light passing through neuronal tissue. These signals are correlated with the measured electrical activity related to the action potential mechanism. Thus, they provide highly useful information about the functioning of neuronal tissue with very high temporal resolution. In this work, the aim was to study the feasibility of a FIOS based activity imaging system with both high temporal and spatial resolutions. In addition, because this method is based purely on the natural functioning of neuronal tissue, it is a very attractive alternative for existing *in vitro* neuroimaging methods, which are based on the use of fluorescence marker substances, which are generally harmful or even toxic.

Although previous research records can be found reporting successful measurements of FIOS events, the experiments have been conducted using only single photodiodes, and thus, no spatial information have been acquired. Additionally, for achieving sufficient SNR, extensive signal averaging has been usually required. Due to the development of photosensitive sensors, FIOS can be acquired with single trials even from the single cultured neurons, which was shown in the measurements conducted by Stepnoski et al. in their photodiode measurements [**19**]. However, recently developed high performance digital imaging sensors should allow also FIOS detection. These sensors provide the missing spatial resolution compared to single photodiode measurements. This would be a major improvement, because spatial information of the action potential signaling mechanism is highly important for example for studying the information processing in the neuronal networks and for the assessment of neuronal network activity without electrophysiological measurements, e.g., for high throughput compound screening in drug development. These specific applications were the primary motivations behind this thesis.

The functioning of neuronal networks, which were used as specimen in this thesis, was electrically measured with MEA technique. The MEA itself is a relatively new measurement method, which also provides spatial information due to the tens of micro-

electrodes placed in the form of an array on which the cells are cultured. Although the MEA provides spatial measuring resolution, it is quite limited because the microelectrodes cannot separate the electrical signals from the individual cells in the vicinity of the electrodes. However, the MEA technique provides excellent opportunity to develop this new neuroimaging method, because the data can be utilized to verify the imaging based activity analysis results. In addition, the MEA technique allows simultaneous microscope observations, because the MEA dishes are manufactured from transparent glass. Due to this, and considering the fact that the microscope used in the observations was equipped with a high performance digital CCD imaging sensor, actually one of the most sensitive sensors available for microscope applications, the starting points for the development task of this new neuroimaging method were close to ideal.

Conducting the measurements was however not straightforward. At the beginning, a lot of effort was needed to get familiar with the measuring devices, and especially to find out how to combine electrical and imaging measurements in a way that these two different data types could be reliable compared. Also, even after thorough literature search, no prior research utilizing similar imaging equipment could be found. Thus, there was no a priori information on the necessary system setup or measurement device parameters. Although the measurement routines became relatively established, the bigger problems were related to issues concerning the studied specimen themselves, and the condition of the imaging equipment. First of all, more specimens with high neuronal activity would have been needed for the work. Additionally the fact that, the specimens were exhibiting neuronal activity only spontaneously, and that there were strict requirements of how long they could be measured at a time without harming the cells, limited the amount of the relevant data to be analyzed.

Unfortunately, analyzing the acquired data failed to detect the FIOS events from the studied neuronal networks. Ultimately the small amount of the data was not the reason for this failing. The imaging devices, mostly the microscope, were in such condition that the acquired image data contained large artifacts due to the highly unstable microscope illumination, which rendered the data ultimately relatively useless.

Regardless of the failing of the measurements, I strongly believe that the outcomes of this thesis can be utilized in future work for conducting the measurements successfully, and thus succeed in developing the proposed novel neuroimaging method, which was the ultimate purpose of this thesis. Large part of this thesis focused to describe the theory behind the optical signals and the devices that can be used in their detection. This did not only provide the knowledge of the requirements considering the detection devices, but especially the knowledge, which can be utilized to optimize and thus dramatically improve the signal acquisition and detection.

The requirements for the detection task and especially how it can be optimized were discussed thoroughly in the end of the results chapter. These requirements are briefly summarized also here. Although an easily available optical device, an optical microscope can be used for the optical image acquisition for this neuroimaging method, it is

highly important to modify the microscope so that the image is created by mainly the light affected by the FIOS mechanisms. By rejecting the background light not affected by the FIOS mechanisms, the SNR of the detected FIOS is directly improved. Regardless of the microscope techniques used to reject the background light intensity, most important is to guarantee that the light source of the microscope provides as stable illumination profile as possible. Considering the digital image formation, one of the key requirements is the frame rate of the imaging sensor, which should achieve a frame rate of the order of thousands of fps. Additionally, the sensitivity and the dynamic range of the sensor should be as high as possible, which are achieved by minimizing the noise contribution in the image formation process.

As for the final conclusion for this thesis, it is highly probable that this neuroimaging method can be developed successfully, because feasibility of the FIOS based imaging has been shown in existing literature. Basically, the only difference between the method proposed in this work and those in the literature is that the single photodiode element is replaced with a digital imaging sensor, which offers both high temporal and spatial resolutions. By learning from the problems we faced in our measurements, and understanding the theory behind this imaging method, the task should not be impossible.

When successfully developed, this method would be extremely useful in experimental neurosciences without excluding the possible *in vivo* clinical applications. At least in my opinion, the proposed future work is well worth of pursuing.

8. REFERENCES

[1] D. K. Hill and R. D. Keynes, "Opacity changes in stimulated nerve," *The Journal of Physiology*, vol. 108, no. 3, pp. 278-281, 1949.

[2] E. N. Marieb, *Essentials of Human Anatomy & Physiology*, 8th ed., San Francisco, Pearson Education, Inc., 2006.

[3] M. F. Bear, B. W. Connors, and M. A. Paradiso, *Neuroscience: Exploring the brain*, 2nd ed., Baltimore, Lippincott Williams & Wilkins, 2001.

[4] J. V. Pelt, I. Vajda, P. Sa Wolters, M. A. Corner, and G. J. A. Ramakers, "Dynamics and plasticity in developing neuronal networks in vitro," in *Development, dynamics and pathology of neuronal networks: From molecules to functional circuits*, J. V. Pelt, M. Kamermans, C. N. Levelt, A. V. Ooyen, G. J. A. Ramakers and P. R. Roelfsema, Eds. Amsterdam, Elsevier, 2004.

[5] T. J. Heikkilä L. Ylä-Outinen, J. M. A. Tanskanen, R. S. Lappalainen, H. Skottman, R. Suuronen, J. E. Mikkonen, J. A. K. Hyttinen, and S. Narkilahti, "Human embryonic stem cell-derived neuronal cells form spontaneously active neuronal networks in vitro," *Experimental Neurology*, vol. 218, no. 1, p. 109-116, 2009.

[6] F. O. Morin, Y. Takamura, and E. Tamiya, "Investigating neuronal activity with planar microelectrode arrays: Achievements and new perspectives," *Journal of Bioscience and Bioengineering*, vol. 100, no. 2, pp. 131-143, 2005.

[7] G. Jing, Y. Yao, M. Gnerlich, S. Perry, and S. Tatic-Lucica, "Towards a multi-electrode array (MEA) system for patterned neural networks," *Procedia Chemistry*, vol. 1, no. 1, p. 329-332, 2009.

[8] A. S. Holik, "Optical microscopy," in *Encyclopedia of Materials: Science and Technology*, K. H. J. Buschow, R. W. Cahn, M. C. Flemings and B. Ilschner, Eds. Amsterdam, Elsevier, 2001.

[9] Nikon Microscopy. Phase contrast microscopy [WWW]. [Cited 10.4.2010]. Available: http://www.microscopyu.com/articles/phasecontrast/phasemicroscopy.html.

[10] Nikon Microscopy. Polarized light microscopy [WWW]. [Cited 12.5.2010]. Available: http://www.microscopyu.com/articles/polarized/polarizedintro.html.

[11] H. D. Young and R. A. Freedman, *University physics with modern physics*, 10th ed., San Francisco**,** Addison-Wesley, 2000.

[12] D. R. Mendoza, "An analysis of CCD camera noise and its effect on pressure sensitive paint instrumentation system signal-to-noise ratio," in *Rec. Int. Congr. Instrumentation in Aerospace Simulation Facilities.*, 1997, pp. 22-29.

[13] Nikon Microscopy. Fundamentals of digital imaging [WWW]. [Cited 25.8.2010]. Available: http://www.microscopyu.com/articles/digitalimaging/ccdintro.html.

[14] Andor Technology. Learning center, CCD binning. [Cited 15.7.2010]. Available: http://www.andor.com/learning/digital_cameras/?docid=320.

[15] B. G. Kornreich, "The patch clamp technique: Principles and technical considerations," *Journal of Veterinary Cardiology*, vol. 9, no. 1, pp. 25-37, 2007.

[16] P. Gogan, I. Schmiedel-Jakob, Y. Chitti, and S. Tyc-Dumont, "Fluorescence imaging of local membrane electric fields during the excitation of single neurons in culture," *Biophysical Journal*, vol. 69, no. 2, pp. 299-310, 1995.

[17] K. Buchheim, O. Wessel, H. Siegmund, S. Schuchmann, and H. Meierkord, "Processes and components participating in the generation of intrinsic optical signal changes in vitro," *European Journal of Neuroscience*, vol. 22, no. 1, pp. 125-132, 2005.

[18] L. B. Cohen, B. Hille, and R. D. Keynes, "Changes in axon birefringence during the action potential," *The Journal of Physiology*, vol. 211, no. 2, pp. 495-515, 1970.

[19] R. A. Stepnoski, A. LaPorta, F. Raccuia-Behling, G. E. Blonder, R. E. Slusher and D. Kleinfeld, "Noninvasive detection of changes in membrane potential in cultured neurons by light scattering," *Proc. Nat. Academy of Sciences of the United States of America*, vol. 88, no. 21, pp. 9382-9386, 1991.

[20] C. Fang-Yen and M. S. Feld, "Intrinsic optical signals in neural tissues: Measurements, mechanisms, and applications," in *New Approaches in Biomedical Spectroscopy*, K. Kneipp, R. Aroca, H. Kneipp and E. Wentrup-Byrne, Eds. Oxford, Oxford University Press, 2007.

[21] A. Zepeda, C. Arias, and F. Sengpiel, "Optical imaging of intrinsic signals: Recent developments in the methodology and its applications," *Journal of Neuroscience Methods*, vol. 136, no. 1, pp. 1-21, 2004.

[22] V. S. Hollis, T. Binzoni, and D. T. Delpy, "Noninvasive monitoring of brain tissue temperature by near-infrared spectroscopy," *Proc. SPIE Optical Tomography and Spectroscopy of Tissue IV*, vol. 4250, p. 470-481, 2001.

[23] J. Beuthan, O. Minet, J. Helfmann, M. Herrig, and G. Müller, "The spatial variation of the refractive index in biological cells," *Physics in Medicine and Biology*, vol. 41, no. 3, pp. 369-382, 1996.

[24] D. Kleinfeld and A. LaPorta, "Detection of action potentials in vitro by changes in refractive index," in *Light scattering imaging of neural tissue function*, D. M. Rector and J. S. George, Eds. New Jersey**,** The Humana Press, Inc., 2003.

[25] A. LaPorta and D. Kleinfeld, "Interferometric detection of action potentials in vitro," in *Imaging in neuroscience and development: A laboratory manual*, R. Yuste and A. Konnerth, Eds. New York**,** Cold Spring Harbor Laboratory Press, 2005.

[26] X. C. Yao, A. Foust, D. M. Rector, B. Barrowes, and J. S. George, "Cross-polarized reflected light measurement of fast optical responses associated with neural activation," *Biophysical Journal*, vol. 88, no. 6, p. 4170-4177, 2005.

[27] D. M. Rector and A. J. Foust, "Optically teasing apart neural swelling and depolarization," *Neuroscience*, vol. 145, no. 3, pp. 887-899, 2007.

[28] X. C. Yao, D. M. Rector, and J. S. George, "Optical lever recording of displacements from activated lobster nerve bundles and Nitella internodes," *Applied Optics*, vol. 42, no. 16, pp. 2972-2978, 2003.

[29] D. Landowne, "Molecular motion underlying activation and inactivation of sodium channels in squid giant axons," *The Journal of Membrane Biology*, vol. 88, no. 2, pp. 173-185, 1985.

[30] K. M. Carter, J. S. George and D. M. Rector, "Simultaneous birefringence and scattered light measurements reveal anatomical features in isolated crustacean nerve," *Journal of Neuroscience Methods*, vol. 135, no. 1, pp. 9-16, 2004.

[31] Andor Technology. Learning center, cropped sensor mode in Andor cameras [WWW]. [Cited 10.8.2010]. Available: http://www.andor.com/learning/digital_cameras/?docid=794.

[32] T. Fawcett, "*ROC graphs: Notes and practical considerations for researchers,"* HP Laboratories, Tech. Rep. HPL-2003-4, 2004.

[33] Nikon Microscopy. Immersion oil and refractive index [WWW]. [Cited 12.11.2010]. Available: http://www.microscopyu.com/tutorials/java/objectives/immersion/index.html.

APPENDIX 1: NEURONAL CELL DIFFERENTIATION AND CULTURING

In this thesis study, we used hESCs differentiated towards neuronal cells. The hESCs are cells that have potential to develop into any cell type found in human body. Due to this property, these cells have huge potential in wide range of research and regenerative medicine. [**5**]

Considering the cell culture preparation process, the neuronal cells are first differentiated from the hESCs through a differentiation process, and thereafter plated and cultured on the MEA dishes for the measurement purposes. Briefly, in the differentiation process, clusters of hESC were cultured 4 to 5 weeks in medium that supported neuronal differentiation. After this period, the hESC clusters formed cell aggregates that consisted of early stage neuronal cells. After the differentiation process, the hESC derived neuronal cell aggregates were seeded on the MEA dishes and cultured in medium which further supported neuronal growth and maturation. [**5**]

After seeding to the MEA dishes, the neuronal cells used in this study were cultured approximately 6-8 weeks prior to the measurements. If cultured for longer periods, neuronal cells tended to grow into very large and dense cell layers on the MEA dishes so that it was not possible to get them properly in focus and imaged with our microscope and imaging equipment. In addition, after certain maturation time, the neuronal cultures tended to decrease their electrophysiological activity. Thus, the most appropriate timing for the imaging measurements was right after the cells had started to exhibit spontaneous electrophysiological activity, which was about 1 to 2 weeks after the seeding. During these first weeks after the seeding, the neuronal cell cultures were active, but not yet grown to dense cell layers, which was optimal for the imaging measurements. However, depending the activity and growth, the neuronal cell cultures were usually cultured for approximately the aforementioned 6-8 weeks.

APPENDIX 2: MICROSCOPE IMAGES

Images shown in this Appendix 2 are taken from the imaging experiments conducted during the measurements related to this thesis. However, these images are not used in the analyzing process, because they are random images captured during configuration of the imaging setup and monitoring of the cell cultures. From the following images, clear differences can be seen in the image quality.

Figure A shows an image captured with brightfield illumination and 40x oil immersion objective. Single cells and cell structures are clearly seen with high details and quality. Clear difference can be seen by comparing this with Figure B and Figure C. Figure B shows brightfield microscopy image captured with 40x objective without oil immersion. Figure C shows polarized light microscopy image captured using 20x objective (no oil immersion, no 40x image available), which have the worst image quality due to the incompatible polarizing filters with the microscope condenser and objective lenses.

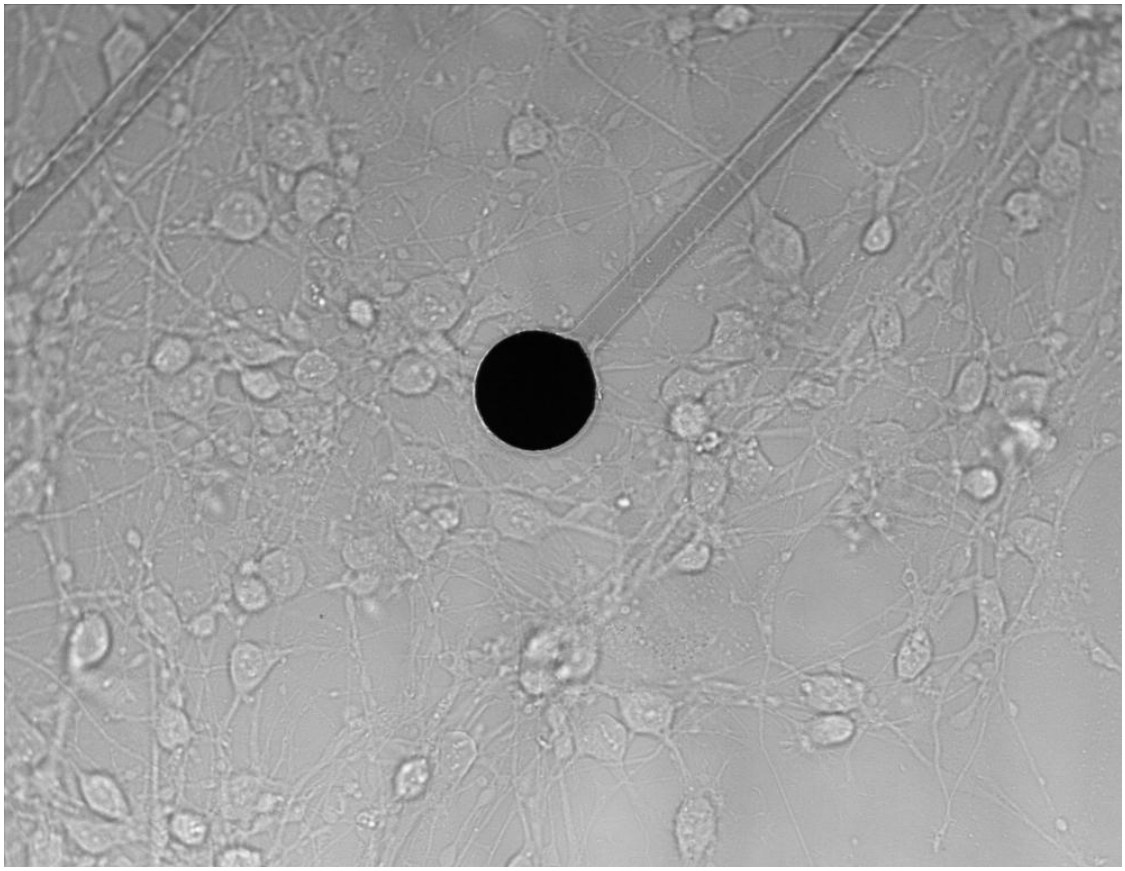

Figure A. *Brightfield microscopy image captured with 40x oil immersion objective.*

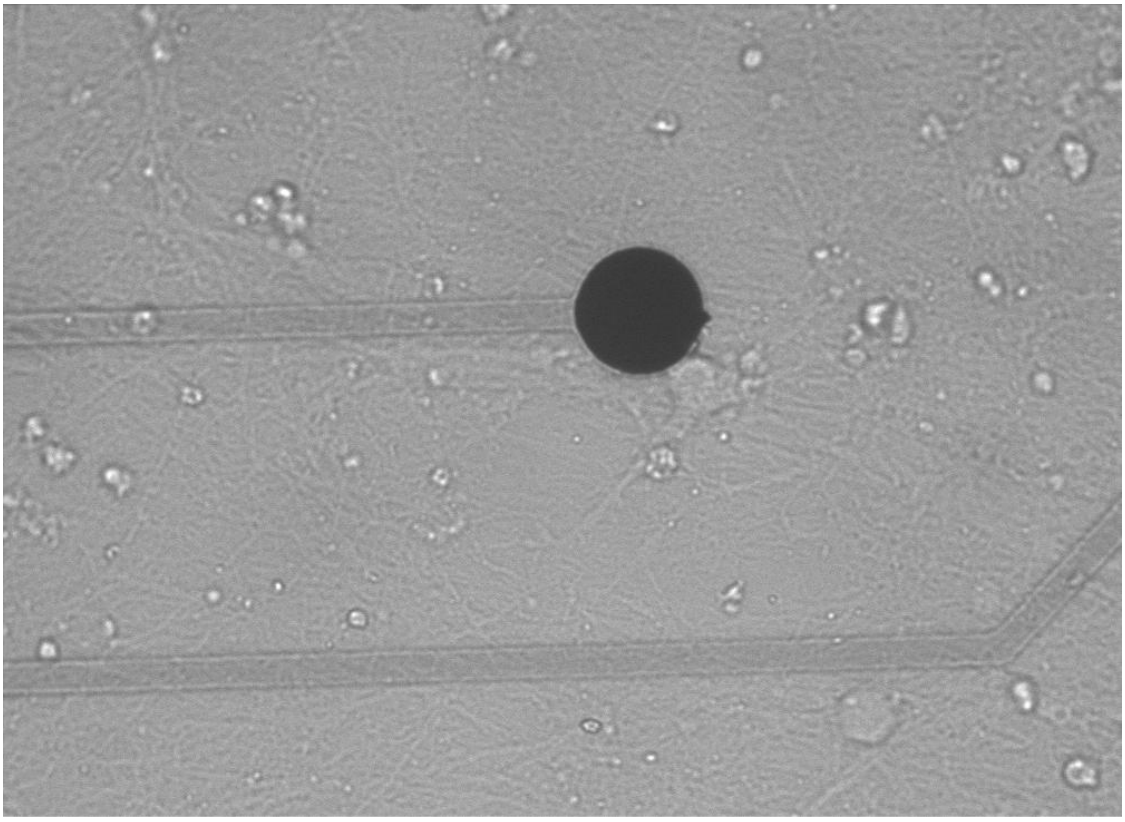

Figure B. *Brightfield microscopy image captured with 40x objective without oil immersion.*

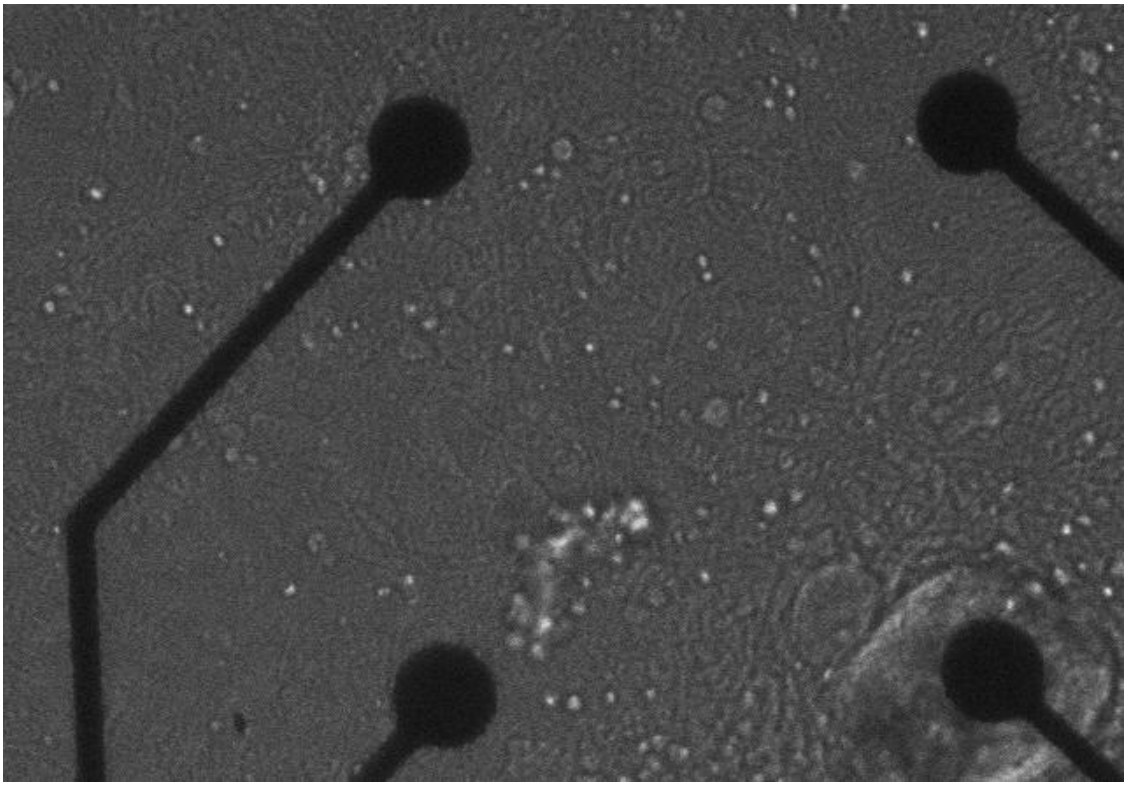

Figure C. *Polarized light microscopy image captured with 20x objective without oil immersion.*